AGU Advances

Key Points:
- Significant global depletion of redox-sensitive trace metals during the early Toarcian may have affected marine microbial ecology
- Estimated organic carbon burial during Toarcian Oceanic Anoxic Event significantly larger than previous estimations for carbon release
- The traditional oceanic anoxic event interval likely associated with greatest extent of euxinia

Supporting Information:

Supporting Information may be found in the online version of this article.

Correspondence to:

T. R. Them,
themtr@cofc.edu

Peer Review The peer review history for this article is available as a PDF in the Supporting Information.

Author Contributions:
Conceptualization: T. R. Them, J. D. Owens
Data curation: T. R. Them, J. D. Owens
Formal analysis: T. R. Them, J. D. Owens
Funding acquisition: J. D. Owens, B. C. Gill

Reduced Marine Molybdenum Inventory Related to Enhanced Organic Carbon Burial and an Expansion of Reducing Environments in the Toarcian (Early Jurassic) Oceans

T. R. Them II[1,2] , J. D. Owens[2] , S. M. Marroquín[3] , A. H. Caruthers[4], J. P. Trabucho Alexandre[5] , and B. C. Gill[6]

[1]Department of Geology and Environmental Geosciences, College of Charleston, Charleston, SC, USA, [2]Department of Earth, Ocean and Atmospheric Science, National High Magnetic Field Laboratory, Florida State University, Tallahassee, FL, USA, [3]Division of Geological and Planetary Sciences, California Institute of Technology, Pasadena, CA, USA, [4]Department of Geological and Environmental Sciences, Western Michigan University, Kalamazoo, MI, USA, [5]Department of Earth Sciences, Universiteit Utrecht, Utrecht, The Netherlands, [6]Department of Geosciences, Virginia Polytechnic Institute and State University, Blacksburg, VA, USA

Abstract Many metals present in trace concentrations in the oceans are sensitive to reduction and oxidation reactions (termed redox-sensitive trace metals or RSTMs) and can therefore be affected during intervals of expanded oceanic anoxia and euxinia (anoxic and sulfidic waters). These RSTMs are important micronutrients; and their availability plays a significant role in controlling metabolic pathways and therefore ecosystem structure. Understanding the links to ecosystem restructuring and potential collapse is important since past deoxygenation events are associated with biological turnover. The Early Jurassic Toarcian Oceanic Anoxic Event (T-OAE) was one such event. We focus on the RSTM molybdenum (Mo), important in the nitrogen cycle, from a basin transect where local redox conditions permit the tracking of the marine reservoir of Mo. Mo enrichments start to decline in the Pliensbachian, continue to decline in the early Toarcian, drop precipitously during the T-OAE interval, and remain low afterward before a protracted increase toward the initial values seen in the Pliensbachian. From a compilation of available data, we estimate that ∼41 Gt of Mo was buried during the T-OAE using a range of possible flux estimates. Given the known correlations of Mo with total organic carbon, the estimated burial of organic carbon during the T-OAE interval was ∼244,000 Gt. This requires a minimum of 3.25% of the ocean floor to be covered by euxinic waters. Finally, we suggest that the intervals traditionally classified as OAEs are associated with the greatest extent of euxinia.

Plain Language Summary Marine metal availability in low amounts is important for organisms that use sunlight to produce energy; thus, a significant reduction in their availability would have profound impacts on the base of marine ecosystems. Using sedimentary molybdenum (Mo) concentrations from a unique region of the Panthalassan (ancient Pacific) superocean, we have reconstructed the marine Mo contents of the global oceans, for the first time, across the Early Jurassic Pliensbachian-Toarcian mass extinction and the Toarcian Oceanic Anoxic Event (T-OAE). We document a significant decrease in the availability of this bioessential trace metal during this time interval, which may have contributed to the observed marine mass extinction. Using our new Mo data, we calculated the amount of organic carbon (OC) buried in the oceans and compared it with previous estimations of carbon release that occurred during the T-OAE. Our new estimates suggest that much more OC was buried than previously estimated. If our modern oceans continue to lose oxygen at high rates, then the future oceans may experience another catastrophic reorganization of the marine ecosystem structure due to not only oxygen loss, but also major decreases in bioessential trace metals.

1. Introduction

1.1. Oceanic Anoxic Events and Redox-Sensitive Trace Metals

Oceanic anoxic events (OAEs) have historically been recognized by organic matter-rich deposition in marine environments across several basins (e.g., Schlanger & Jenkyns, 1976), which were suggested to represent an expansion of marine anoxia. The stratigraphic extent of an OAE is typically defined by a carbon isotope excursion (CIE) that represents a perturbation to the global carbon cycle. These excursions are found worldwide. Often, but not always, an OAE is characterized by locally elevated organic carbon (OC) concentrations in sedimentary

Investigation: T. R. Them, J. D. Owens, S. M. Marroquín, A. H. Caruthers, B. C. Gill
Methodology: T. R. Them, J. D. Owens
Project Administration: J. D. Owens
Resources: J. D. Owens
Supervision: J. D. Owens
Visualization: T. R. Them
Writing – original draft: T. R. Them, J. D. Owens, S. M. Marroquín, A. H. Caruthers, J. P. Trabucho Alexandre, B. C. Gill
Writing – review & editing: T. R. Them, J. D. Owens, A. H. Caruthers, J. P. Trabucho Alexandre, B. C. Gill

deposits (as reviewed by Jenkyns (2010), Kemp, Suan, et al. (2022), and Owens et al. (2018)). Studying OAEs may provide an understanding of the link between past events of environmental change and biological evolution (e.g., increased turnover, mass extinctions, etc.). Although OAEs are, as their name suggests, thought to be associated with major changes in the extent of marine redox conditions on a global scale, recently new proxies have been developed to more accurately track the degree of deoxygenation and its temporal extent (e.g., Bowman et al., 2019; Newby et al., 2021; Ostrander et al., 2017; Them et al., 2018; see Owens, 2019)—suggesting reducing condition are not limited to only the OAE interval.

Understanding the link between the availability of redox-sensitive trace metals (RSTMs) and biological evolution in the marine system across ancient extinction events is also becoming increasingly critical to our society. The modern global ocean has lost more than 2% of its dissolved oxygen over the past 50 years linked to climatic warming (e.g., Schmidtko et al., 2017). Shoaling of hypoxic regions of the open oceans can lead to habitat compression for aerobic organisms (e.g., Köhn et al., 2022). Projections of O_2 loss suggest that this trend will continue for at least centuries (e.g., Keeling et al., 2010; Long et al., 2016). Additionally, it has been documented that O_2 loss has a rapid negative influence on aerobic ecosystem structures in the oceans (e.g., Breitburg et al., 2018; Diaz & Rosenberg, 2008; many others). In the modern marine environment, a healthy and fully functioning phytoplankton-driven ecosystem is directly controlled by nutrient availability in the oxygenated upper ocean, which includes many RSTMs (e.g., Morel & Price, 2003). Redox-sensitive trace metals (e.g., Mo, V, Cu, and others) are necessary for several metabolic processes including photosynthesis, and these requirements are thought to have remained relatively constant throughout biological evolution over much of geologic time (e.g., Reinhard et al., 2013).

Bioessential RSTMs such as Mo also have a wide range of individual chemical and redox sensitivities (Anbar & Knoll, 2002; Lyons et al., 2014; Reinhard et al., 2013; T. J. Algeo & Maynard, 2004), and many RSTMs are enriched in reducing marine or estuarine sediments or sediments deposited under anoxic to euxinic (anoxic and sulfidic) water columns (e.g., Bennett & Canfield, 2020; Tribovillard et al., 2006). In the modern oxygenated ocean, for example, ~35% to 50% of molybdenum (Mo) is removed via adsorption onto manganese oxyhydroxides (Mn-oxides) in marine sediments (e.g., Bertine & Turekian, 1973; Morford & Emerson, 1999; Shimmield & Price, 1986; Takematsu et al., 1985). Molybdenum accumulation in these environments is slow, but much of the Mo lost from the oceans today leaves through this sink since these sediments cover a large portion of the modern seafloor (Bertine & Turekian, 1973; Scott & Lyons, 2012). On the other hand, ~50% to 65% of Mo is removed in the oceans through scavenging via organic matter or sulfides in sulfidic water columns or sediments (e.g., Scott et al., 2008; cf. Chappaz et al., 2014). This occurs because Mo transforms into a particle-reactive oxy thiomolybdate ($MoS_nO^{2-}_{(4-n)}$) under sulfidic conditions (e.g., Erickson & Helz, 2000). The seafloor covered by euxinic waters represent only a small (<<1%) portion of the modern global oceans, however note that the burial efficiency (i.e., the ability of an OC compound to withstand remineralization) in these environments is much greater than in their oxygenated counterparts (Canfield, 1994).

Molybdenum concentrations in sediments deposited under euxinic waters often reach values >100s ppm, whereas sediments with sulfide restricted only to pore waters have Mo concentrations <~30 ppm (Scott & Lyons, 2012). Molybdenum concentrations between ~30 and 100 ppm can also result from natural (e.g., seasonal, annual, etc.) variability in water column redox conditions (e.g., Scott & Lyons, 2012 and references therein). Varying sedimentation rates and diffusion rates of Mo and S into sediments can also cause Mo concentrations to overlap (<25 ppm) from fully oxygenated to euxinic end-member environments (e.g., Hardisty et al., 2018). Therefore, enrichments of Mo have been used as proxies for locally reducing conditions due to its efficient removal in these environments (e.g., Bennett & Canfield, 2020; Chappaz et al., 2014; Hardisty et al., 2018; T. J. Algeo & Liu, 2020; Tribovillard et al., 2006; many others).

While there has been much research focused on resolving long-term changes in marine RSTM inventories during the Archean and Proterozoic (e.g., Lyons et al., 2009, 2014; Partin et al., 2013; Reinhard et al., 2013; many others), less is known regarding the global fluctuations during intervals of marine deoxygenation in the Phanerozoic. It has long been speculated that ancient time intervals associated with widespread marine anoxia and organic matter deposition have the capacity to draw down the RSTM marine inventory (e.g., Emerson & Huestead, 1991). For example, Algeo (2004) suggested that Late Devonian RSTM records in the Appalachian Basin indicate a global depletion of the marine RSTM reservoirs driven by widespread postoxic (e.g., non-sulfidic anoxia) conditions during an interval of increased OC burial. Subsequently, drawdown of the marine reservoirs has been
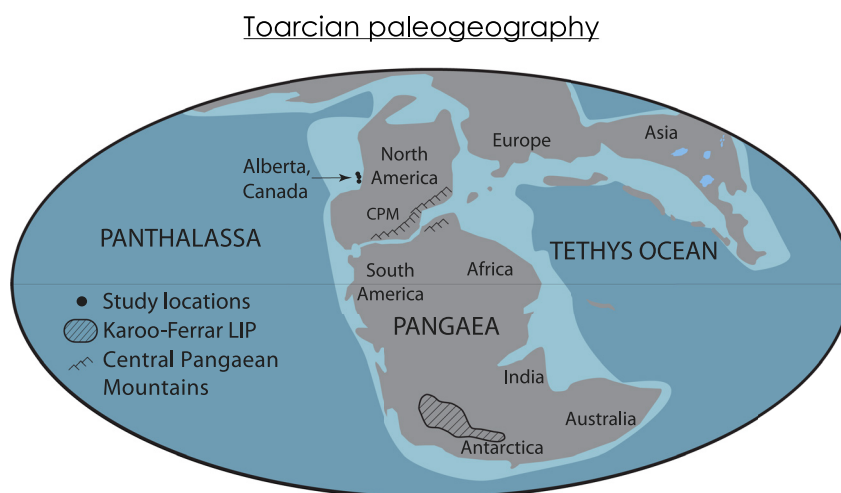
Toarcian paleogeography

Figure 1. Global paleogeography of the early Toarcian (modified from Scotese (2001), Them, Gill, Caruthers, et al. (2017), and Them, Gill, Selby, et al. (2017)). Black circles represent study sites. Hatched outline in southern Africa and Antarctica represents location and extent of Karoo-Ferrar large igneous province. Dark gray represents landmasses, light blue represents shallow seas, and dark blue represents open oceans. CPM represents the Central Pangean Mountains. Reprinted with permission from Scotese (2001).

suggested to have occurred during several other events during the Phanerozoic including OAE-2 in the Cretaceous (Dickson, Saker-Clark, et al., 2017; Goldberg et al., 2016; Owens et al., 2016), the Lau Event in the Silurian (Bowman et al., 2021) and the SPICE event in the Cambrian (Gill, Lyons, Young, et al., 2011; Gill et al., 2021). Furthermore, the global marine RSTM inventory may have been more susceptible to increases in marine anoxia (and therefore the bioavailability of RSTMs) as the marine reservoir may have been substantially lower than the modern reservoir before these events (e.g., Bowman et al., 2021; Gill, Lyons, Young, et al., 2011; Gill et al., 2021; Owens et al., 2016; T. Algeo, 2004). The drawdown of marine RSTMs, especially Mo, during OAEs may therefore have affected the basal ecology of the oceans, with the possibility of a larger impact on eukaryotes due to their higher RSTM metabolic requirements (e.g., Liu et al., 2021; Owens et al., 2016).

1.2. The Early Jurassic Toarcian Oceanic Anoxic Event

Perhaps the most catastrophic Mesozoic OAE, in terms of environmental change and extinction, was the Early Jurassic Toarcian Oceanic Anoxic Event (T-OAE; ~183 Ma; see Figure 1). Current understanding suggests that it was most likely triggered by the emplacement of the Karoo-Ferrar large igneous province (LIP; e.g., Pálfy & Smith, 2000), whereby volcanogenic outgassing caused a host of biogeochemical changes and a cascade of environmental feedbacks including massive outgassing of carbon from marine and terrestrial ^{12}C-enriched pools (e.g., Beerling & Brentnall, 2007; Hesselbo et al., 2000; Them, Gill, Caruthers, et al., 2017; Ruebsam et al., 2019); a significant increase in strength of the hydrologic cycle, global weathering, and soil erosion (e.g., Chen et al., 2021; Izumi et al., 2018; Kemp et al., 2020; Liu et al., 2020; Percival et al., 2016; Them, Gill, Selby, et al., 2017; Them et al., 2019; Xu et al., 2018); widespread marine anoxia and euxinia (e.g., Dickson, Gill, et al., 2017; French et al., 2014; Gill, Lyons, & Jenkyns, 2011; Liu et al., 2021; Schouten et al., 2000; Schwark & Frimmel, 2004; Them et al., 2018; van Breugal et al., 2006); a transition to bacterial-dominated microbial ecosystems at some locations (e.g., Liu et al., 2021); and a global marine mass extinction (e.g., Caruthers et al., 2013; Dera et al., 2010; Harries & Little, 1999).

As a result, the T-OAE produced a geochemically unique signature in the stratigraphic record, with one of its hallmark characteristics being the widespread deposition of OC-rich sediments throughout many European successions and other locations around the world (e.g., Jenkyns, 1988, 2010; Them, Gill, Caruthers, et al., 2017; and others). The T-OAE is classically defined by a large (~2‰ to 12‰), globally observed, negative carbon isotope excursion (N-CIE) that occurs in lower Toarcian marine and terrestrial sediments that may interrupt a somewhat cryptic broad positive CIE (e.g., Hesselbo et al., 2000; Ikeda et al., 2018; Jenkyns & Clayton, 1997; Jin et al., 2020; Liu et al., 2020, 2021; Them, Gill, Caruthers, et al., 2017; Them et al., 2018). It has recently

been suggested, however, that globally significant increases of expanded bottom-water anoxia began at the Pliensbachian-Toarcian (Pl-To) boundary, well before (and was sustained well after) the classically defined OAE (Them et al., 2018), concomitant with the beginning of the main phase of the multi-phased extinction event (e.g., Caruthers et al., 2013). This is significant because it suggests that widespread post-oxia or marine anoxia occurred over a much longer timeframe (>1 Ma), and therefore its potential influence on marine RSTM inventories may have also been protracted.

Currently, it is debated whether there were (a) global changes in marine redox during the T-OAE and (b) a global drawdown of the RSTM inventory during the T-OAE (see McArthur, 2019; McArthur et al., 2008; Remírez & Algeo, 2020b). Interestingly, both debates are linked to the power and reliability of geochemical proxies used to reconstruct environmental change. Some have suggested that "evidence for a global OAE during the Early Toarcian is weak" (e.g., Remírez & Algeo, 2020b), and others have proposed that the term "Toarcian oceanic anoxic event be abandoned" (e.g., McArthur, 2019). This first debate (i.e., point (a)) is related to the observation that not all Toarcian locations experienced local anoxia (whether in the water column or sediments) during the OAE. Many authors focus on the OC concentration of sediments to infer local anoxia. This, however, cannot be used as direct evidence of anoxia as total organic carbon (TOC) contents are not reliable indicator of bottom water redox and it is common to have similar TOC contents in sediments deposited under fully oxygenated to euxinic water columns (e.g., Canfield, 1994; Hartnett et al., 1998; Kemp, Suan, et al., 2022; Owens et al., 2018). Other methods such as sedimentary iron speciation (in siliciclastic-dominated rocks) or iodine/calcium values (in OC-lean carbonates) represent proxies that more explicitly track local redox changes and have shown the full range of redox conditions spanning the T-OAE (e.g., Lu et al., 2010; Them et al., 2018). More importantly, it has rarely been proposed that all areas of the oceans experienced anoxic or reducing conditions during OAEs (but see Monteiro et al., 2012; Wang et al., 2021), and therefore it should not be surprising that many regions (especially shallow areas within the mixed layer of the oceans, or central open-ocean gyres) remained relatively well-oxygenated across these events; the view that the entire ocean, or even most of the ocean, became anoxic represents one of the most common misconceptions regarding marine redox evolution across OAEs (see Monteiro et al., 2012; Wang et al., 2021).

For the early Toarcian interval, however, novel sulfur, thallium, and Mo isotope data argue for an increased geographic extent of anoxic and euxinic bottom waters, likely on a global scale (e.g., within multiple ocean basins; Dickson, Gill, et al., 2017; Dickson, Saker-Clark, et al., 2017; Gill, Lyons, & Jenkyns, 2011; Them et al., 2018), but again not the entire ocean. The thallium isotope data from Them et al. (2018) also suggest initial deoxygenation occurred before the traditional T-OAE interval in the late Pliensbachian and extended well after it into the middle Toarcian. The debate on whether a global drawdown of the RSTM inventory occurred during the T-OAE revolves around the fact that no studies have been conducted at sites where locally anoxic/euxinic redox conditions were sustained before, during, and after the event (e.g., Chen et al., 2021; Kemp, Chen, et al., 2022; McArthur, 2019; McArthur et al., 2008; Remírez & Algeo, 2020a, 2020b; Thibault et al., 2018; Wang et al., 2021). These conditions are fundamental to track the global RSTM marine reservoir (e.g., Figure 2, e.g., Owens et al., 2016; see Figure 2).

To date, studies centered on the Toarcian RSTM inventory predominantly focus on European successions representing a variety of depositional environments within an epeiric sea (e.g., Dickson, Gill, et al., 2017; Dickson, Saker-Clark, et al., 2017 and references therein; Wang et al., 2021). Much attention has been placed on RSTM data from the Cleveland Basin succession (Yorkshire, UK; representing the northwest European epeiric seaway) during the T-OAE, which has been the focal point of debate concerning the global versus local/regional nature of the RSTM systematics (McArthur, 2019; McArthur et al., 2008; Hesselbo et al., 2020; Remírez & Algeo, 2020a, 2020b; Thibault et al., 2018). Within this work, it was recently argued that the global Mo reservoir decreased during the T-OAE interval (e.g., Thibault et al., 2018), whereas others have suggested these changes in RSTMs across the T-OAE are not globally extensive and are rather the product of local hydrographic restriction (e.g., McArthur, 2019; McArthur et al., 2008; Remírez & Algeo, 2020b). Furthermore, metal isotope records from Cleveland Basin have been attributed to local, not global, changes in water mass chemistry (e.g., Cohen et al., 2004; Dickson, Gill, et al., 2017; Nielsen et al., 2011; Pearce et al., 2008). Unfortunately, other Toarcian RSTM records (e.g., other locations within the European epeiric sea, Japan, and South America) do not have the long-term local redox conditions required to more directly track global RSTM marine inventories (e.g., Baroni et al., 2018; Fantasia, Föllmi, Adatte, Bernárdez, et al., 2018; Fantasia, Föllmi, Adatte, Spangenberg, et al., 2018; Hermoso et al., 2013; Kemp, Chen, et al., 2022; Kemp & Izumi, 2014; see Figure 2; see Data Set S1). This
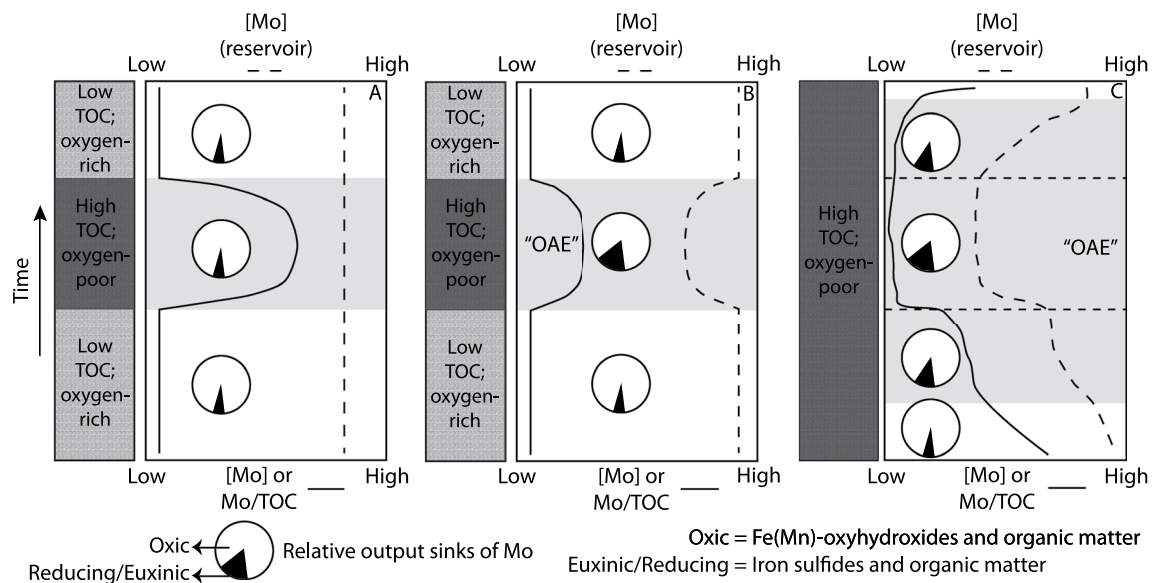
Figure 2. Idealized molybdenum (Mo) and Mo/total organic carbon (TOC) systematics in the marine realm. The bottom panel (solid line) represents local Mo concentrations and Mo/TOC values measured from fine-grained, siliciclastic-dominated sedimentary succession. The top panel (dashed line) represents the global marine Mo reservoir. The pie chart represents the relative contribution of oxic and reducing environments with respect to burial of Mo within the global ocean. (a) In this non-Oceanic Anoxic Event (OAE) scenario, anoxic, organic matter-rich sediments are sandwiched between oxygenated, organic matter-poor sediments. Locally, sedimentary Mo values increase during anoxic sedimentation, but there is little to no change in the marine Mo reservoir because anoxia and organic carbon (OC) burial is not widespread. (b) In this OAE scenario, anoxic, organic matter-rich sediments are deposited between oxygenated, organic matter-poor sediments. Locally, sedimentary Mo values increase only slightly during anoxic sedimentation, and there is a synchronous decrease in the global marine Mo reservoir size because anoxia and OC burial is widespread. (c) In this OAE scenario, anoxic, organic matter-rich sediments are deposited during the entire study interval in an open-ocean (Cariaco-like) basin. Locally sedimentary Mo values decrease as Mo and OC burial increases before the classic OAE interval. After the OAE interval, local sedimentary Mo values begin to increase and the global Mo reservoir begins to recover as widespread sedimentation under anoxic conditions decreases. *Note that these idealized TM records come from fine-grained, siliciclastic-dominated sediments as the proxy has not been calibrated for limestones. Furthermore, in these idealized records, low-TOC intervals are associated with oxygenated settings, whereas high-TOC intervals are associated with anoxic settings. In reality, both low- and high-TOC sediments can be deposited in either redox regime, and it is necessary to generate ancillary local redox proxies (e.g., iron speciation) to distinguish between them. It is also important to note that Mo chemostratigraphy from highly restricted depositional environments (e.g., T-OAE Yorkshire record) may be similar to Scenario C, thus constituting inappropriate evidence for interpreting global changes in marine chemistry.

reinforces the need for coeval data outside the European epeiric sea and Tethys Ocean and from locations that have stable, reducing redox conditions before, during, and after the event.

In this contribution, we present Mo data across the upper Pliensbachian–middle Toarcian interval, including the classic T-OAE interval, from multiple localities along a basin transect within the Western Canada Sedimentary Basin (WCSB). The Lower Jurassic Fernie Formation was deposited in a shelf-slope environment of westernmost Laurentia with an accretionary arc to the west, and geological evidence suggests that this region maintained strong connections with the open-ocean deep waters of Panthalassa throughout the Early Jurassic (e.g., Păna et al., 2019; Poulton & Aitken, 1989; Them, Gill, Caruthers, et al., 2017). Furthermore, this region experienced relatively stable, locally reducing redox conditions throughout the study interval (e.g., Them et al., 2018, Figure 1). We report data generated across the basin transect (southeast-northwest; see Them et al., 2019) to resolve variation in the global Mo inventory. We then use a compilation of Mo data to estimate both Mo and OC burial during the study interval with implications for the area of the seafloor worldwide that experienced euxinic conditions and budgets for the global carbon cycle over the T-OAE.

2. Materials and Methods

Splits of powdered samples from previous geochemical studies (Them, Gill, Caruthers, et al., 2017; Them, Gill, Selby, et al., 2017; Them et al., 2018; 2019) were analyzed for their elemental compositions (e.g., Al and Mo) at the National High Magnetic Field Laboratory at Florida State University. Carbon isotope, TOC, and iron speciation data used in this study are reported elsewhere (e.g., Them, Gill, Caruthers, et al., 2017; Them, Gill, Selby, et al., 2017; Them et al., 2018). Samples were dissolved using a standard total digestion method with
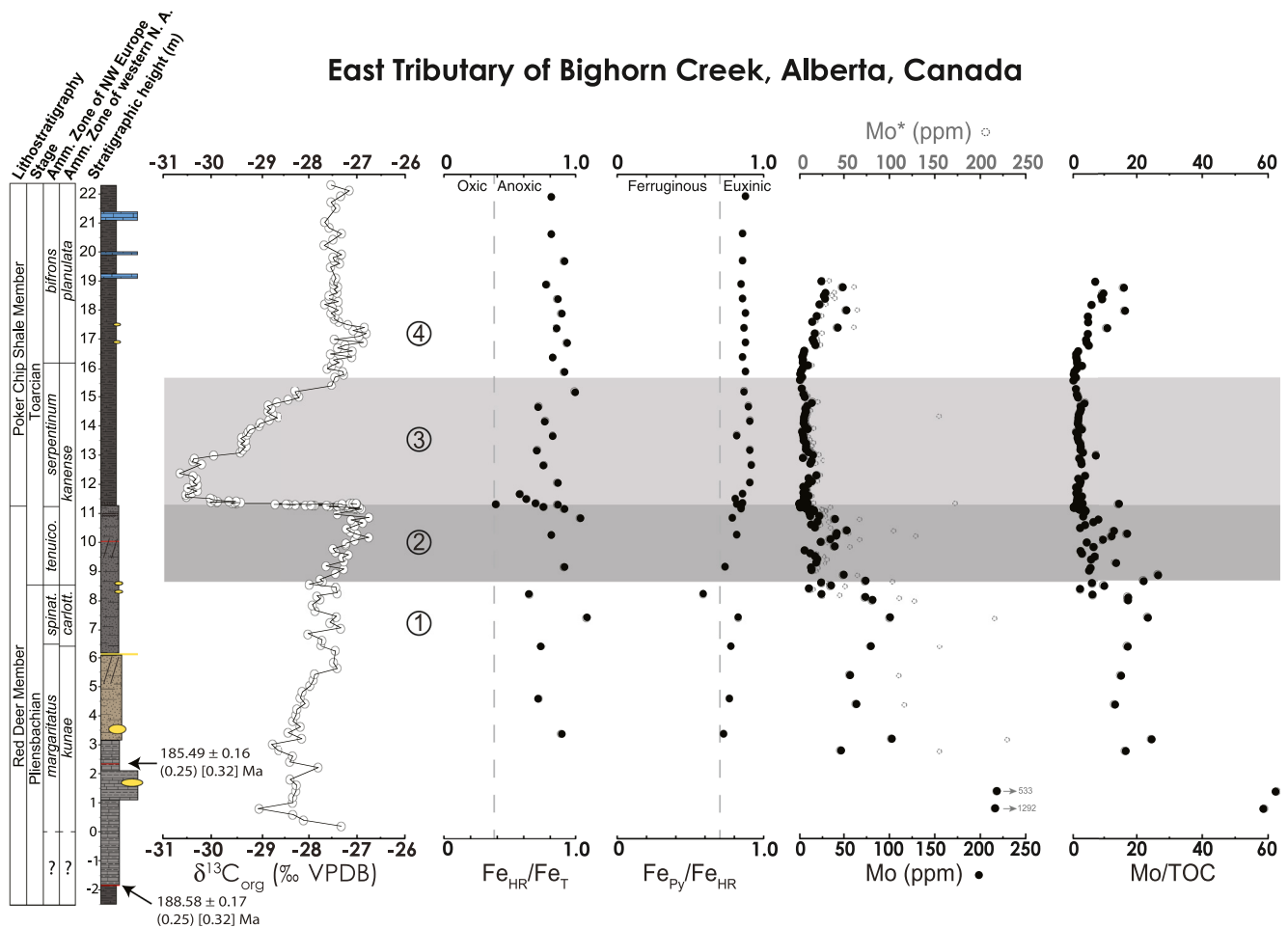
Figure 3. Chemostratigraphy from proximal, shallower-water East Tributary of Bighorn Creek, Alberta. $\delta^{13}C_{org}$, organic carbon isotopic composition from Them, Gill, Caruthers, et al. (2017); TOC = total organic carbon from Them, Gill, Caruthers, et al. (2017); iron speciation data from Them et al. (2018). Lithostratigraphic members of the Fernie Formation, stages of the Jurassic, and ammonite zonations for both northwestern Europe and western North American shown to the left of the stratigraphic column (refer to Them, Gill, Caruthers, et al. (2017) and Them et al. (2018) for their placements). The Mo data have been corrected to account for carbonate dilution, which is variable. Time slices are as follows: 1 = late Pliensbachian; 2 = Pl-To boundary to base of Toarcian Oceanic Anoxic Event (T-OAE) negative carbon isotope excursion (N-CIE) (dark gray box); 3 = T-OAE N-CIE interval (medium gray box); 4 = post-T-OAE N-CIE.

HCl-HNO_3-HF in a CEM MARS 5 and 6 microwave digestion system with trace metal clean vials and acids. After complete sample digestion, each sample was re-dissolved in 2% HNO_3 solution and analyzed using an Agilent 7500cs ICP-MS. Internal standards and spikes were used to measure elemental abundances and correct the samples for instrument drift. External standards (USGS SCo-1 and SDO-1) were used and have values within 3% for each reported element. Duplicate samples also have a reproducibility of $\pm 3\%$ or less for all elements. Procedural blanks were below detection limits for all reported elements.

3. Elemental Data and Results

Data were collected from three stratigraphic sections representing an upper Pliensbachian–middle Toarcian basin transect of the Fernie Formation in the WCSB. All study sites show elevated Mo/Al and Mo/TOC values leading up to the Pl-To boundary (Figures 3–5). In all the records, there is a general decline in Mo concentrations ([Mo]) at the Pl-To boundary, and another significant decrease at the onset of the traditional T-OAE interval, that is, the interval that contains the N-CIE (Figures 3–5). At the proximal East Tributary location where detailed biostratigraphic data exist (Them, Gill, Caruthers, et al., 2017), [Mo] do not return to pre-excursion levels directly after the T-OAE N-CIE, but they begin a slow rise in the *Planulata* ammonite Zone (Figure 3). These trends are also observed using Mo/TOC (ppm/wt% $\times 10^{-4}$) values and Mo enrichment factors.
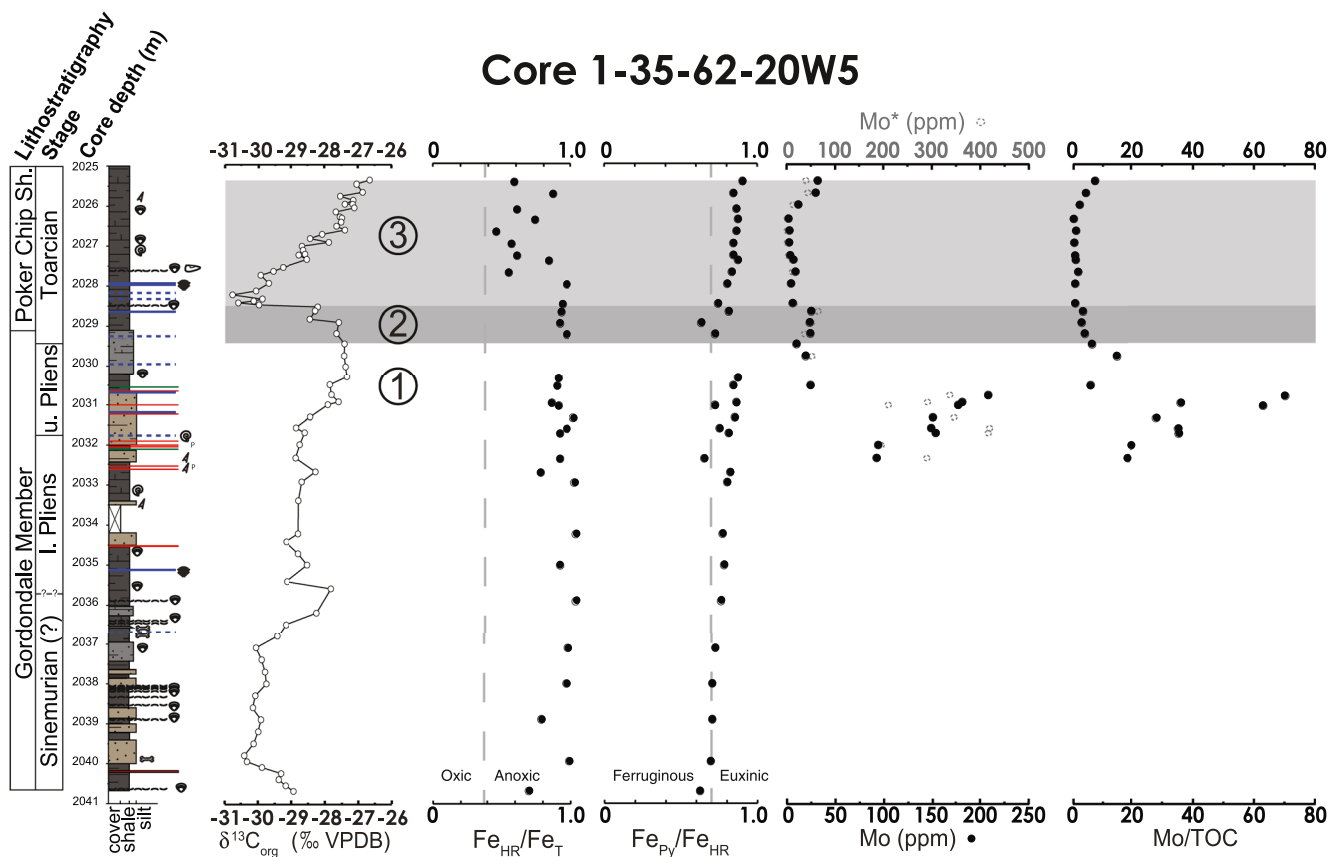
Figure 4. Chemostratigraphy from intermediate drill core 1-35-62-20W5, Alberta. $\delta^{13}C_{org}$, organic carbon isotopic composition from Them et al. (2018); TOC = total organic carbon from Them et al. (2018); iron speciation data from Them et al. (2018). Lithostratigraphic members of the Fernie Formation and stages of the Jurassic shown to the left of the stratigraphic column (refer to Them et al. (2018) for their placement). The molybdenum data have been corrected to account for carbonate dilution, which is variable. Time slices are as follows: 1 = late Pliensbachian; 2 = Pl-To boundary to base of Toarcian Oceanic Anoxic Event (T-OAE) negative carbon isotope excursion (N-CIE) (dark gray box); and 3 = T-OAE N-CIE interval (medium gray box).

Similar to the [Mo] trend, Mo/TOC values show a long-term decrease at the two more proximal locations (East Tributary and core 1-35-62-20W5) in the upper Pliensbachian before quickly declining in the lower Toarcian and reaching their lowest values during the N-CIE interval. At East Tributary where sample resolution is highest, there is a transient spike in Mo/TOC values at the Pl-To boundary. At the most distal locality (core 6-32-75-5W6), Mo/TOC values show a long-term decrease leading up to the Pl-To boundary and remain low during the N-CIE interval. Approximately 1 m above the N-CIE interval, Mo/TOC values begin to rise in the lower *Planulata* ammonite Zone, similar to the East Tributary site, and eventually reach pre-N-CIE levels (~10–20). An increase in Mo/Al and Mo/TOC values is also observed after the T-OAE N-CIE interval in the distal locality during the middle Toarcian (Figure 5). The upper Pliensbachian and lower Toarcian are more condensed stratigraphically at this location and therefore some of the short-term [Mo] perturbations observed from the other locations (if they represent basinwide or global Mo perturbations) may not be captured here due to the sample resolution.

4. Discussion

The setting and redox proxy data for the WCSB basin transect suggest this is an ideal location for tracking the global marine inventory of Mo (see explanation below). First, these locations represent open marine environments along the western margin of Laurentia (easternmost Panthalassan Ocean) with a relatively representative and biostratigraphically complete upper Pliensbachian-middle Toarcian section (e.g., Poulton & Aitken, 1989; Them, Gill, Caruthers, et al., 2017; Them, Gill, Selby, et al., 2017; Them et al., 2018; Păna et al., 2019). Second, these sections have been used to successfully reconstruct global changes in other isotope systems (e.g., C, Os, and Tl; e.g., Them, Gill, Caruthers, et al., 2017; Them, Gill, Selby, et al., 2017; Them et al., 2018) even as global sea
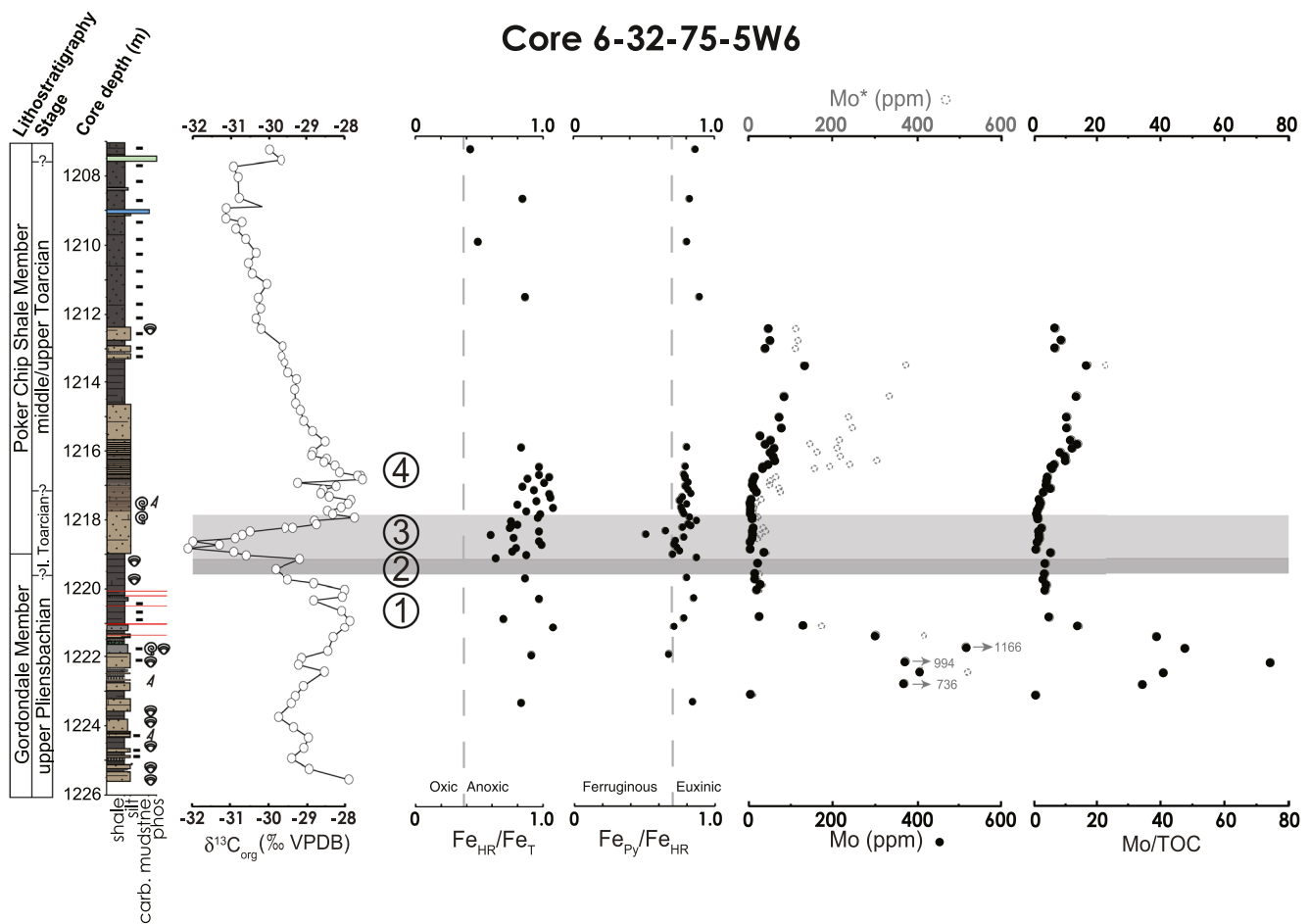
Figure 5. Chemostratigraphy from distal, deeper-water drill core 6-32-75-5W6, Alberta. $\delta^{13}C_{org}$, organic carbon isotopic composition from Them et al. (2018); TOC = total organic carbon from Them et al. (2018); iron speciation data from Them et al. (2018). Lithostratigraphic members of the Fernie Formation and stages of the Jurassic shown to the left of the stratigraphic column (refer to Them et al., 2018 for their placements). The [Mo] data have been corrected to account for carbonate dilution, which is variable. Time slices are as follows: 1 = late Pliensbachian; 2 = Pl-To boundary to base of Toarcian Oceanic Anoxic Event (T-OAE) negative carbon isotope excursion (N-CIE) (dark gray box); 3 = T-OAE N-CIE interval (medium gray box); 4 = post-T-OAE N-CIE.

level fluctuated (e.g., Hallam, 2001). Third, deposition at these locations occurred under predominantly anoxic and euxinic conditions as determined using the iron speciation redox proxy (e.g., Them et al., 2018), which allows us to also discount changes in local redox as a driver of the Mo records. Here, we discuss this new Mo data set in light of: (a) the suspected global changes in Mo inventory across the T-OAE; (b) the novel use of sedimentary Mo/TOC data and their role in estimating both Mo and OC burial rates (e.g., Owens et al., 2018), and estimates of percent global seafloor experiencing euxinic conditions during the Toarcian (e.g., Reinhard et al., 2013); and finally (c) a re-evaluation of the OAE concept, in context of our new estimates of OC burial and existing estimates for the release of carbon necessary to produce the T-OAE N-CIE along with previously published redox data.

4.1. Pliensbachian-Toarcian North American Mo Trends

In the upper Pliensbachian, the average Mo/TOC value from the three study sites is ~25 (range of ~22–30), which is similar to the modern euxinic Cariaco Basin (~25; e.g., T. J. Algeo & Lyons, 2006), suggesting a large global marine Mo inventory similar to today (if sediment accumulation rates were similar). The Cariaco Basin yields high Mo/TOC values because Mo is efficiently removed from the upper water column, which is continuously renewed by Mo-rich, open-ocean water (e.g., T. J. Algeo & Lyons, 2006). These average Mo/TOC values drop to 4.4 (Pl-To boundary to N-CIE; range of 3.4–5.6) and 1.7 (N-CIE; range of ~1.1 to 2.1), before rising to 7.6 (post-N-CIE; range of ~7.3 to 7.9). These trends are similar to that of Yorkshire, which has been argued to be the result of changing basin restriction (e.g., McArthur, 2019; McArthur et al., 2008; Remírez & Algeo, 2020b) due

to the similarity with the modern Black Sea Mo/TOC values (e.g., T. J. Algeo & Lyons, 2006). The Black Sea has depressed Mo/TOC values (~4) because the renewal rate of Mo-rich waters from the Mediterranean Sea is slower than the rate at which Mo is moved from the euxinic water column in the basin (e.g., T. J. Algeo & Lyons, 2006). Based on previous studies of the WCSB, this region maintained strong connections with the open-ocean deep waters of Panthalassa throughout the Early Jurassic (e.g., Păna et al., 2019; Poulton & Aitken, 1989; Them, Gill, Caruthers, et al., 2017; Them, Gill, Selby, et al., 2017), thus there is no supporting evidence to suggest basin restriction played a role in the Mo/TOC data or interpretations.

The Mo concentration and other metal isotope data challenge the supposition that there were no changes in global redox during the T-OAE. They also suggest that marine oxygen concentrations did not fully recover to background values on a global scale at the end of the traditionally defined OAE, or N-CIE, interval. Eastern Panthalassan sedimentary Mo and carbonate-corrected Mo (Mo-cc) concentrations decrease coevally with changes in Tl isotopes at the Pl-To boundary and Tl and S isotopes at the T-OAE N-CIE (Figures 3–5; e.g., Gill, Lyons, & Jenkyns, 2011; Newton et al., 2011; Them et al., 2018). These metal isotope records have been interpreted as evidence of widespread/increased marine deoxygenation (Them et al., 2018) and euxinia or pyrite burial (e.g., Gill, Lyons, & Jenkyns, 2011; Newton et al., 2011). Considered in isolation, some of these absolute Mo concentrations observed during this interval could be interpreted to represent locally non-reducing conditions (e.g., Hardisty et al., 2018); Fe speciation data, however, suggest locally persistent euxinic bottom-water conditions in this basin during this interval (Them et al., 2018), leaving changes in marine reservoir of Mo the likely interpretation for the Canadian Mo records. Notably, both the S- and Tl-isotope systems remain perturbed well after the classically defined T-OAE interval as defined by the N-CIE (Gill, Lyons, & Jenkyns, 2011; Newton et al., 2011; Them et al., 2018), and as the new Mo records from the WCSB also show depletion, it is probable that the oceans remained in a more reducing state, relative to the late Pliensbachian, after the classic T-OAE interval.

These new data sets from eastern Panthalassa suggest a decreasing marine Mo reservoir beginning near the Pl-To boundary followed by a continued global drawdown of Mo during and after the normally defined T-OAE interval (N-CIE; see Them et al., 2018). As the area of postoxic and euxinic marine environments increased, along with or related to more organic matter deposition in sediments, the burial flux of Mo out of the system would have also increased, thereby decreasing the dissolved marine reservoir (e.g., Emerson & Huestead, 1991; T. Algeo, 2004). These factors would have increased the burial efficiency and therefore sequestration of bioessential nutrients in the oceans (e.g., Reinhard et al., 2013). This is consistent with a stepwise sequence of increased organic matter burial (e.g., Jenkyns, 1988; Them, Gill, Caruthers, et al., 2017) and expanded deoxygenation (Them et al., 2018) followed by a global increase in pyrite burial during and after the classic T-OAE interval (e.g., Gill, Lyons, & Jenkyns, 2011).

Carbon isotope values slowly decrease during the middle to upper Toarcian (e.g., Jenkyns et al., 2001; Them et al., 2018) when Mo/TOC values start to increase. Using linear sedimentation rates from East Tributary and core 6-32-75-5W6, the first rise in Mo/TOC values in the *Planulata* ammonite Zone is contemporaneous (~182.4 Ma; see Data Set S1). The large increase in Mo/TOC values from core 6-32-75-5W6 occurs ~182 Ma (~1 Ma after the classic T-OAE interval), but this later Mo/TOC trend from East Tributary cannot be resolved as the Mo data set ends at ~182.1 Ma based on linear sedimentation rates.

As the ocean remained in this relatively deoxygenated state, the enhanced preservation and burial of organic matter continued to occur, which is observed in several locations around the world after the N-CIE interval including shallow and deep-sea environments (e.g., Ikeda et al., 2018; Them, Gill, Caruthers, et al., 2017; Them et al., 2018). The low Mo and Mo/TOC values were likely driven by a smaller Mo reservoir, which was sustained by increased output fluxes (i.e., organic matter-rich deposition; see Chappaz et al., 2014), rather than a transient and enhanced Mo burial episode during the classic T-OAE interval followed by an increasing marine Mo reservoir over several hundred thousand years as observed in core 6-32-75-5W6 (residence time of Mo is ~450 ka in the modern oxygen-replete oceans; Miller et al., 2011). Generally, enhanced OC burial is recognized in the geologic record by either positive CIEs (Kump & Arthur, 1999) and/or widespread black shale deposition (see Jenkyns, 2010). While there is known widespread black shale deposition (Jenkyns, 1988; Them, Gill, Caruthers, et al., 2017), there is not a significant positive CIE in this interval (e.g., Jenkyns & Clayton, 1997; Them et al., 2018). It is possible that this expected outcome may have been muted or offset via continued addition or inputs of isotopically light carbon from multiple sources (e.g., Beerling & Brentnall, 2007; Them, Gill, Caruthers, et al., 2017). Additionally, it is also likely that marine OC burial remained elevated (as was the geographic extent

of bottom-water anoxia), but was declining relative to the T-OAE interval and offset by input of isotopically light carbon, which is supported by lower-resolution thallium isotope data that extend into the middle Toarcian (e.g., Them et al., 2018). Although the potential role of OC burial in the deep sea setting is difficult to resolve given the dearth of preserved Toarcian deep-sea successions (see Kemp, Suan, et al., 2022), even small changes in OC burial in the deep sea could be an important factor in the global carbon cycle given the larger percentage of the total ocean floor encompassed by these environments (e.g., Owens et al., 2018). As the Panthalassan Ocean was by far the largest ocean basin during the study interval (and the entire Phanerozoic), it is likely that this location represented a significant locus of OC burial.

These data suggest that the Toarcian Mo record was controlled by the relative output flux into sediments. Molybdenum concentrations from distal drill core 6-32-75-5W6 begin increasing approximately 1 m above the N-CIE, suggesting that some regions of the oceans experienced decreased OC burial and post-oxia, which decreased RSTE output flux and led to an increased marine reservoir. The increase in Mo/TOC values is also contemporaneous with more depleted $\delta^{13}C$ values (Figure 5), supporting a role for decreasing OC burial rates rather than the replenishment of the Mo reservoir via weathering. On the other hand, continued injections of isotopically light carbon from the Karoo-Ferrar LIP during this time interval and subsequent biogeochemical feedbacks may have sustained more efficient Mo removal (e.g., Greber et al., 2020 and references within). Osmium isotope data suggest decreased weathering rates in the post-N-CIE interval relative to the N-CIE, but still elevated compared to pre-N-CIE values (e.g., Kemp et al., 2020; Percival et al., 2016; Them, Gill, Selby, et al., 2017). Thallium isotope data from this section of the drill core corroborate our interpretation as they suggest a slow increase of global bottom-water oxygenation (Them et al., 2018), which may have affected OC preservation and therefore Mo (and other RSTM) drawdown. These new Mo records from North America are broadly consistent with Mo chemostratigraphy from Dotternhausen, Germany where there is biostratigraphic overlap in the Toarcian and the proper (e.g., fine-grained, reducing, OC-rich) sediments to compare (e.g., Dickson, Gill, et al., 2017). Therefore, these combined records provide compelling evidence that the T-OAE N-CIE global marine Mo reservoir was depleted. As such, a small global marine Mo reservoir in concert with basin restriction likely resulted in the large regional variability of water mass (and therefore sedimentary) Mo concentrations and isotopes observed from several other European basins during the study interval (Chen et al., 2021; Dickson, Gill, et al., 2017; Dickson, Saker-Clark, et al., 2017; McArthur et al., 2008; Pearce et al., 2008; Thibault et al., 2018).

4.2. Estimating Molybdenum and Organic Carbon Burial

These open-ocean Mo records are used here to estimate the amount of Mo buried globally using estimates for local sedimentation rates over the Pl-To interval in the East Tributary section and estimated global weathering rates during the T-OAE N-CIE (e.g., Them, Gill, Selby, et al., 2017; Them et al., 2018; see Data Set S1). After determining the global amount of Mo buried during each respective interval, Mo/TOC values can then be used based on the observed correlation to TOC in different modern basins (e.g., T. J. Algeo & Lyons, 2006) to calculate the amount of OC buried (*sensu* Owens et al., 2018; see Data Set S1). To accomplish this, the Pl-To study interval has been binned into four different time intervals: (a) late Pl to Pl-To boundary; (b) Pl-To boundary to T-OAE N-CIE; (c) T-OAE N-CIE; and (d) post-T-OAE N-CIE (Figure 6).

While Mo abundances have been published from various sections, there are significant challenges with using them to constrain the marine Mo inventory, however, given the potential influences of local hydrographic restriction, facies changes, sedimentary accumulation rates, and redox changes on these records. With these concerns in mind, calculations were conducted based on the Mo and Mo/TOC data from the WCSB transect and then compared to a global compilation of Mo data from various lithologies (see Tables 1–4 and Table S1). The Pl-To boundary is placed at 184 Ma based on magnetic susceptibility data from European strata (e.g., Ait-Itto et al., 2018), and small changes in the absolute date of the Pl-To boundary do not significantly affect our interpretations of Mo or OC burial during each time bin. The duration of the N-CIE is estimated at 500 ka (183.1–182.6 Ma) based on an absolute age date from South America (Sell et al., 2014) and cyclostratigraphic analysis from European epeiric seaway successions (Boulila et al., 2014, 2019) and deep-sea cherts from Panthalassa (Ikeda et al., 2018). Global weathering rates are suggested to have increased by ~200% during this interval based on Os isotope records (lower estimate from Kemp et al., 2020; Percival et al., 2016, Them, Gill, Selby, et al., 2017). Higher estimates also exist (~500% to 800%; e.g., Cohen et al., 2004; Kemp et al., 2020; Them, Gill, Selby, et al., 2017) but are likely unrealistic (see Them, Gill, Selby, et al. (2017) for additional discussion on this point). Sedimentation rates
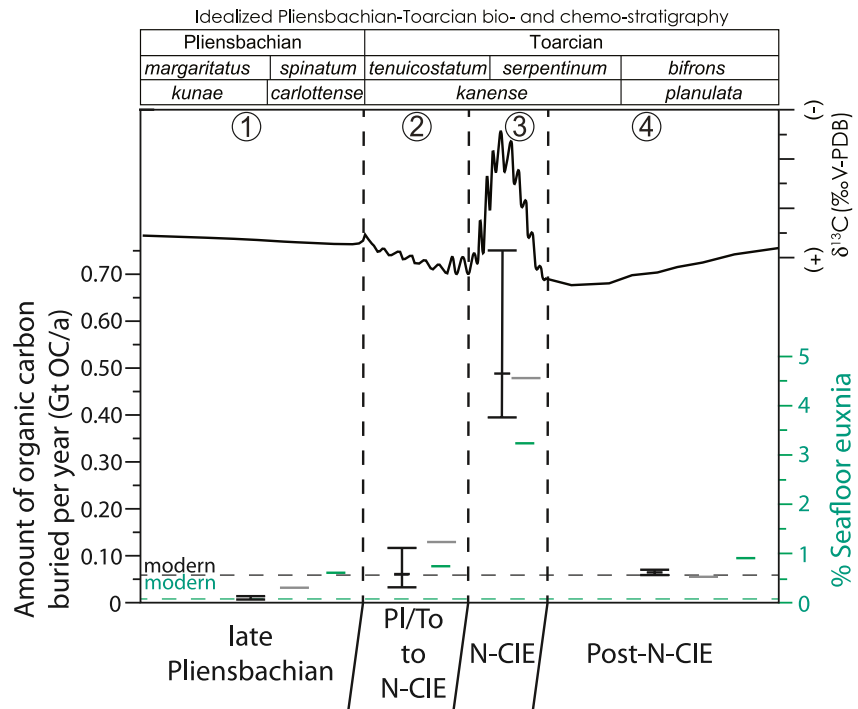
Figure 6. Organic carbon (OC) burial and euxinic area estimations across late Pliensbachian to early Toarcian. The range of OC burial values for each time interval comes from the highest and lowest Mo/total organic carbon (TOC) value from Canada and Germany, with the middle bar representing the average molybdenum (Mo)/TOC value (black lines; see Data Set S1 for these calculations). Gray lines represent global compilation Mo/TOC averages for each time interval. Green values represent the seafloor percentage of euxinia. 1 = late Pliensbachian; 2 = Pl-To boundary to base of Toarcian Oceanic Anoxic Event (T-OAE) negative carbon isotope excursion (N-CIE); 3 = T-OAE N-CIE interval; 4 = post-T-OAE N-CIE.

from the East Tributary section are derived from previous age models (e.g., Them, Gill, Selby, et al., 2017; Them et al., 2018). The post-T-OAE N-CIE sedimentation rates were kept constant relative to the N-CIE rates, as there are no bentonite beds or other absolute age markers that can be used for age constraints, and there is also minimal variation in lithofacies in this interval.

The reduction of the global Mo reservoir size is estimated from the average Mo concentrations from the three Canadian sites for each time bin. The average Mo/TOC values from Canada and Germany were used for the late Pliensbachian, Pl/To boundary to N-CIE, N-CIE, and post-N-CIE intervals of 25, 6, 1.7, and 7.3 ppm/TOC%, respectively. Assuming a modern Mo weathering flux and reservoir size (e.g., Miller et al., 2011) and no change in the global Mo reservoir or weathering rates during the entire study interval, then an average of $\sim 2.97 \times 10^{14}$ mol of Mo (~ 28.5 Gt Mo) is estimated to have been buried during the N-CIE over 500 ka—this provides a background conservative estimate but is not indicative of the observations. Using the Mo/TOC value of 1.7 would estimate a burial of $\sim 1.67 \times 10^{20}$ g OC ($\sim 167,000$ Gt OC or ~ 167 e.g.,) during the N-CIE. Relative

Table 1
Molybdenum and Organic Carbon Burial Estimates for the Pliensbachian-Toarcian Interval

Time bin	Mo ocean (moles)	Mo input (moles/yr)	Duration (Myr)	Total Mo burial (moles)	Average Mo/TOC	Organic carbon burial (Gt)	Organic carbon burial (Gt/yr)
1	1.47E+14	3.00E+08	1.390	5.64E+14	25.0	21,600	0.016
2	1.47E+14	3.00E+08	1.0	4.47E+14	6.0	71,400	0.071
3	1.47E+14	3.00E+08	0.500	2.97E+14	1.7	167,400	0.335
4	1.47E+14	3.00E+08	2.312	8.40E+14	7.3	110,000	0.048

Note. Time bin 1–4 are from Figures 3–6. There is no change in weathering or global marine Mo reservoir size.

Table 2

Molybdenum and Organic Carbon Burial Estimates for the Pliensbachian-Toarcian Interval Accounting for a Drawdown of the Molybdenum Reservoir

Time bin	Mo ocean (moles)	Mo input (moles/yr)	Duration (Myr)	Total Mo burial (moles)	Average Mo/TOC	Organic carbon burial (Gt)	Organic carbon burial (Gt/yr)
1	1.47E+14	3.00E+08	1.390	5.64E+14	25.0	21,600	0.016
2	1.47E+14	3.00E+08	1.0	4.25E+14[a]	6.0	67,900	0.068
3	2.20E+13	6.00E+08	0.500	4.32E+14[b]	1.7	244,000	0.488
4	1.47E+13	4.50E+08	2.312	1.06E+15	7.3	138,700	0.060

Note. Time bin 1–4 are from Figures 3–6.

[a]An 85% drawdown of marine Mo reservoir relative to the previous time slice. [b]A 90% drawdown of marine Mo reservoir relative to Age 1.

to the late Pliensbachian, an excess of ∼160,000 Gt OC was buried, or ∼0.32 Gt OC per year, equating to OC burial rates that were ∼19.5× higher.

Observed data, however, suggest there is a reduction of the global Mo reservoir at the Pl/To boundary and N-CIE by 85% and then to 90%, respectively. A Mo reservoir 85%–90% lower than the modern, assuming that the starting reservoir was similar to today (107 nM), approaches the N-fixation threshold of 10 nM (Glass et al., 2010, 2012); significantly, a smaller starting reservoir only decreases the final reservoir size. An increase in weathering rates (2×) during the N-CIE (Percival et al., 2016; Them, Gill, Selby, et al., 2017) would increase the Mo and TOC burial estimates during the interval. Using these observations, ∼4.3 × 10¹⁴ mol of Mo (∼41 Gt Mo) would have been buried during the T-OAE N-CIE interval, which requires that ∼2.44 × 10²⁰ g OC (∼244,000 Gt OC or ∼244 Eg [e.g.,]) were buried during the T-OAE N-CIE interval (Figures 6 and 7, Table 2; see Mo and Mo/TOC compilation in Data Set S1)—burying an excess of ∼236 Eg of OC, or ∼0.47 Gt OC per year, relative to the late Pliensbachian. Importantly, this equates to OC burial rates that were ∼31× higher.

These estimates, which are sensitive to the exact duration of the time bin, could be less if the duration of the T-OAE N-CIE was reduced; the 500-ka duration, however, is in the lower end of current estimates. If the N-CIE interval was 1 Ma in duration, then ∼413 Eg of OC would have been buried, but the rate of carbon burial (∼0.40 Gt OC per year) would have been less due to the nonlinear relationship. While these calculations yield a large range of burial estimates, they do provide independent constraints on the OC burial during the T-OAE that can be used to compare to classic modeling of the C cycle based on the carbon isotope record (see Section 4.5).

Next, we perform this same process using carbonate-corrected Mo concentrations to remove the effects that any carbonate dilution may have on the records, as Mo is not associated with a carbonate host phase mineral (see Figures 2–4). The Mo/TOC values do not change, but the estimated global Mo reservoir drawdown across the Pl/To boundary and N-CIE intervals changes to ∼90% and ∼95%, respectively. Assuming that weathering doubled, then ∼42 Gt Mo and ∼248 Eg of OC were buried. This equates to an excess of ∼0.48 Gt OC per year relative to

Table 3

Molybdenum and Organic Carbon Burial Estimates for the Pliensbachian-Toarcian Interval From Canada and Dotternhausen Using Carbonate-Corrected Mo Concentrations

Time bin	Mo ocean (moles)	Mo input (moles/yr)	Duration (Myr)	Total Mo burial (moles)	Average Mo/TOC	Organic carbon burial (Gt)	Organic carbon burial (Gt/yr)
1	1.47E+14	3.00E+08	1.390	5.64E+14	25.0	21,600	0.016
2	1.47E+14	3.00E+08	1.0	4.32E+14[a]	6.0	69,100	0.069
3	1.47E+13	6.00E+08	0.500	4.39E+14[b]	1.7	247,900	0.496
4	7.33E+12	4.50E+08	2.312	1.05E+15	7.3	137,700	0.060

Note. Time bin 1–4 are from Figures 3–6.

[a]A 90% drawdown of marine Mo reservoir relative to the previous time slice. [b]A 95% drawdown of marine Mo reservoir relative to Age 1.

Table 4
Molybdenum and Organic Carbon Burial Estimate for the Pliensbachian-Toarcian Interval From the Global Compilation

Time bin	Mo ocean (moles)	Mo input (moles/yr)	Duration (Myr)	Total Mo burial (moles)	Average Mo/TOC	Organic carbon burial (Gt)	Organic carbon burial (Gt/yr)
1	1.47E+14	3.00E+08	1.390	5.64E+14	12.2	44,300	0.032
2	1.47E+14	3.00E+08	1.0	4.10E+14[a]	3.1	126,900	0.127
3	3.66E+13	6.00E+08	0.500	4.25E+14[b]	1.7	239,600	0.479
4	2.20E+13	4.50E+08	2.312	1.06E+15	8.2	124,300	0.054

Note. Time bin 1–4 are from Figures 3–6.
[a]A 75% drawdown of marine Mo reservoir relative to the previous time slice. [b]An 85% drawdown of marine Mo reservoir relative to Age 1.

the late Pliensbachian. It is clear that the difference between the Mo and OC burial estimations derived from the bulk Mo concentrations and carbonate-corrected Mo concentrations is minimal.

This was also performed using the global compilation of Pl-To Mo data (see Data Set S1), which includes restricted basins and many locations deposited under variable local redox conditions over the study interval with varying lithologies. As previously discussed, these locations are less reliable for constraining global redox conditions. Nevertheless, these calculations resulted in OC burial rates that are ~15× higher during the N-CIE interval relative to the late Pliesnbachian. For this exercise, average Mo/TOC values of 12.2, 3.1, 1.7, and 8.2 ppm/TOC% from were used for the late Pliensbachian, Pl/To boundary to N-CIE, N-CIE, and post-N-CIE intervals, respectively. Based on the Mo concentrations, global decreases in the Mo reservoir were calculated to be 75% and 85% during the Pl/To boundary and N-CIE interval, respectively.

It has also recently been suggested that increased thermal maturity may lead to artificial increases in Mo/TOC values due to the preferential loss of OC (e.g., Ardakani et al., 2016; Dickson et al., 2020, 2022). If these results
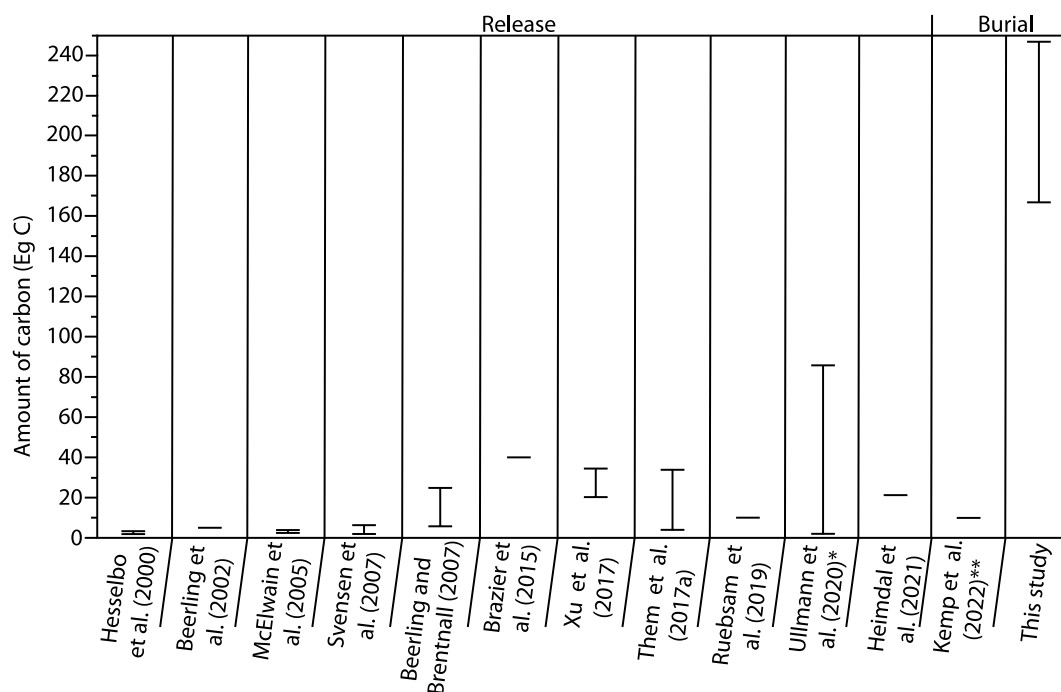

Figure 7. Organic carbon (OC) release and burial estimations across the Toarcian Oceanic Anoxic Event (T-OAE) negative carbon isotope excursion (N-CIE). The range of OC burial estimates is the result of using the average OC burial rates from Canada under constant and 2× increase in Mo weathering during the classic T-OAE interval. *Note that the large range from Ullmann et al. (2020) is the result of modeling how much C release would reproduce the T-OAE N-CIE using different starting magnitudes for the marine C reservoir. **This estimation represents a minimum value.

universally apply, then the Mo and OC burial estimations (presented in this study) potentially represent maxima. For example, if the Mo/TOC value is doubled due to heating and the loss of 50% of the initial OC (e.g., Dickson et al., 2020), then ~122 Eg of OC would have been buried during the N-CIE interval, which is 50% of the original estimate. Even if all the estimates are reduced by 50% due to post-depositional processes affecting the primary Mo/TOC relationship, OC burial rates during the Toarcian was still significantly higher than in the Pliensbachian, but the relative increase in burial rates do not change because Mo/TOC values increase by a factor of two for all time bins. It is clear, however, that the duration of each time bin and the Mo/TOC values are the most important factors controlling both Mo and OC burial estimates. We stress again that this technique requires unique study sites and depositional conditions for these estimations to be utilized. Using the global Mo database to estimate Mo and OC burial, which includes restricted basins and locations with variable local redox conditions, leads to an underestimation of ~50%.

4.3. Estimating % Seafloor Euxinia

It is possible to estimate the amount of seafloor that experienced euxinic conditions for each of the Pliensbachian and Toarcian time bins using calculations derived from modern Mo burial fluxes and extent of euxinic regions in the oceans (Reinhard et al., 2013). Using a modern flux of Mo into organic matter and sulfides (1.9×10^7 mol/yr) and the modern area of the ocean covered by euxinic conditions (0.11%), the estimates for the four time bins are as follows: (a) late Pliensbachian = 0.61%; (b) Pl-To boundary to N-CIE = 0.72% (range of 0.63%–0.76% using 75%–90% Mo reservoir drawdown estimations, respectively); (c) N-CIE = 3.26% (range of 3.18%–3.35% using 85%–95% Mo reservoir drawdown estimations with double weathering, respectively); and (d) post-N-CIE = 0.91% (range of 0.88%–0.92% using 85%–95% Mo reservoir drawdown estimations during N-CIE and new steady-state weathering, respectively). It is important to note that these calculations are highly influenced by the modern Black Sea budget (Reinhard et al., 2013) and also presume a constant Mo burial efficiency under euxinic conditions for each time interval. Regardless, these estimates suggest that, relative to the late Pliensbachian, the seafloor area that was covered by euxinic waters during the intervals from Pl-To boundary to N-CIE, N-CIE, and post-N-CIE was ~1.2×, ~5.3×, and ~1.5× higher, respectively. These estimations support other proxy data suggesting that non-sulfidic anoxia during the Toarcian pre-N-CIE interval prevailed before sulfidic and euxinic conditions developed during the N-CIE interval and persisted after the OAE (Gill, Lyons, & Jenkyns, 2011; Newton et al., 2011; Them et al., 2018). These estimates most likely represent minima as the assumption is that redox conditions remained constant in any singular area, but they likely varied through space and time.

4.4. Re-Evaluation of the "OAE"

The concept of the OAE was based upon the stratigraphic manifestation of organic matter-rich sediments from epeiric, epicontinental, and open-ocean locations (see Schlanger & Jenkyns, 1976). These new estimates paired with global redox data suggest that OC burial and reducing conditions in the global ocean likely persisted well before and after the classically defined OAE. Based on our calculations, this prolonged interval of expanded reducing marine conditions may have caused a reduction in the global ocean Mo reservoir by ~90% (Figure 6). Further, the suppressed marine Mo inventory after the T-OAE N-CIE suggests persistent reducing, anoxic, and euxinic environments in some portions of the ocean. Other lines of geochemical evidence of global marine redox changes across the Toarcian also suggest that bottom-water deoxygenation persisted long after the classically defined T-OAE interval based on Tl and S isotopes (Gill, Lyons, & Jenkyns, 2011; Them et al., 2018), concomitant with elevated Mo and OC burial rates (Figure 6). Large regions of the seafloor with high OM contents could have fueled bottom-water anoxia for much longer than the classic T-OAE interval due to high rates of local OC remineralization in sediments (Them et al., 2018).

It is also possible that phosphorus regeneration under anoxic conditions (e.g., Froelich et al., 1979; Ingall & Jahnke, 1994) sustained high primary productivity in the photic zone. This may have resulted in a feedback loop (e.g., increased anoxia—phosphorus regeneration—primary productivity) that maintained increased bottom-water anoxia and pyrite burial for an extended interval after the T-OAE (Gill, Lyons, & Jenkyns, 2011; Them et al., 2018) due to the continued delivery of labile organic matter to bottom water environments and subsequent remineralization. Enhanced weathering and delivery of terrestrial materials also characterized the post-T-OAE N-CIE interval (Kemp et al., 2020; Percival et al., 2016; Them, Gill, Selby, et al., 2017), which may

have helped maintain high levels of primary productivity via addition of bioessential (and limiting) nutrients such as nitrate. For this scenario to be realistic, however, the Karoo-Ferrar LIP would have had to continue to inject significant amounts of C into the atmosphere after the N-CIE interval to fuel elevated rates of chemical weathering. Recent age constraints on the Karoo-Ferrar LIP suggest a main eruptive phase of igneous activity from ~184 to 180 Ma (see Greber et al., 2020 and references within), which supports our interpretations of the marine geochemical record. Elevated seawater temperatures in Europe and increased global weathering rates relative to the pre-N-CIE interval have been suggested during the post-N-CIE interval in the Toarcian (e.g., Them, Gill, Selby, et al., 2017; Ullmann et al., 2020).

These new OC burial estimates for the Pl-To interval can be compared to another Mesozoic OAE. It has recently been suggested that ~70 Eg of OC was buried during Cretaceous OAE-2 over 500 ka (~0.14 Eg/kyr; e.g., Owens et al., 2018). This value is roughly twice that for the interval from Pl-To boundary to N-CIE (~68 Eg OC over 1 Ma or ~0.06 Eg/kyr; Figure 6). This suggests that before the T-OAE N-CIE interval, elevated OC burial may have primed the oceans for a significant OC burial spike (~8×) during later environmental upheavals. The N-CIE interval OC burial rates are ~4× higher than during OAE-2 (e.g., Owens et al., 2018), pointing to a much larger injection of C to the ocean/atmosphere system and/or response of the carbon cycle to LIP volcanism during the Toarcian. This stepped and larger perturbation to the carbon cycle during the Toarcian likely contributed in the multi-phased Pliensbachian-Toarcian mass extinction (e.g., Caruthers et al., 2013; Dera et al., 2010; Harries & Little, 1999), compared to the smaller biotic response during the Cretaceous OAE-2 (e.g., Leckie et al., 2002).

Recent advances in proxy development and their application to Phanerozoic "OAEs" have painted a more nuanced picture of environmental change across these intervals. It appears that increased geographic extents of anoxia or reducing conditions are not only limited to the intervals that contain large-magnitude CIEs, which are generally used to define the bounds of the OAEs. The OAE intervals as currently defined by C isotopes, however, most likely represent the intervals of minimum oceanic oxygen and maximum anoxia and euxinia. Therefore, we suggest that a more valid term that reflects the CIE interval in the oceans, regardless of direction (i.e., positive or negative), is an oceanic euxinic event (OEE). This comports with the redox evolution in the oceans across OAEs (e.g., Gill, Lyons, & Jenkyns, 2011; Ostrander et al., 2017; Owens et al., 2013, 2016; Them et al., 2018). Although the term OAE is widely used, its current definition should be reevaluated in light of these new findings. A more accurate naming system will also need to include environmental change that occurred on land. The term carbon cycle perturbations (CCPs) is useful in that it is more inclusive and also encompasses environmental change that occurs in terrestrial environments and does not require changes in local redox (e.g., Jin et al., 2020; Liu et al., 2020; Xu et al., 2017). Environmental change across these global carbon cycle pertubations may also be applicable to similar intervals across the entire Phanerozoic as evidence for widespread organic matter-rich shales is not required since the deep sea records of these events are generally not well preserved.

4.5. Implications for Ancient Carbon Release Estimations

This exercise for estimating OC burial using the Mo record highlights some potential limitations of estimating C release scenarios based solely on the C isotope record. Importantly, the C isotope record tracks the integrated input and output fluxes of C and any respective isotopic fractionation associated with each process (e.g., Freeman, 2001; Kump & Arthur, 1999). Previous estimations of C release necessary to generate the N-CIE and the increase in pCO_2 (500–1,600 p.p.m.v.; e.g., McElwain et al., 2005; Ruebsam et al., 2020) have ranged from ~1,500 to 87,000 GtC, with the highest value necessitating a much larger initial reservoir size of C in the oceans than is usually assumed (Figure 7). These estimations may have, in general, underestimated the total amount of C released (Figure 7) as they do not account for any synchronous increases in organic matter burial—basics observed with lithology, which would move the C isotope composition of the oceans and atmosphere in the opposite direction. A recent analysis suggests that ~9,000 GtC were buried in shallow seas during the classic T-OAE interval (e.g., Kemp, Suan, et al., 2022). It is unlikely that these high amounts of C would have been available in the exogenic C cycle to bury as OC unless there were significantly higher C input fluxes to the oceans and atmosphere. Therefore, it is likely that the C release (and burial) during the early Toarcian was much greater than currently appreciated, and was most likely associated with protracted Karoo-Ferrar LIP outgassing and potentially other biogeochemical feedbacks.

The outgassing of mantle-derived CO_2 during LIP volcanism is not thought to have solely caused negative CIEs, as the $\delta^{13}C$ value of this CO_2 (~−5‰) would necessitate unreasonable inputs of CO_2 to the atmosphere (e.g.,

Beerling & Brentnall, 2007; Gales et al., 2020 and references therein). It is possible, however, to release a very large amount of mantle C (δ^{13}C = −5‰) and smaller amounts of ^{12}C-enriched C from other sources to cause geologically transient N-CIEs (e.g., Beerling & Brentnall, 2007; Them, Gill, Caruthers, et al., 2017). Previous pCO$_2$ reconstructions using the stomatal index and the difference in the magnitude of the CIE in marine and terrestrial environments argue for an increase in atmospheric pCO$_2$ by 500–800 p.p.m.v. during the T-OAE (e.g., McElwain et al., 2005; Ruebsam et al., 2020), much smaller than expected with the C burial calculated in this study (Figure 7). If current estimations grossly underestimate C release during the early Toarcian, then why do pCO$_2$ reconstructions not suggest higher values? This is reconcilable as the response to elevated greenhouse gas concentrations led to a globally rapid silicate weathering response and increased OC burial leading to marine anoxia, which consumed atmospheric CO$_2$ (e.g., Jenkyns, 1988; Them, Gill, Caruthers, et al., 2017; Them, Gill, Selby, et al., 2017; Them et al., 2018; Kemp et al., 2020). This assumes no net changes in carbonate weathering or precipitation, which impacts pCO$_2$ levels on short timescales. Therefore, atmospheric greenhouse concentrations did not increase more during the T-OAE because the output fluxes sequestered (or buffered) much of this outgassed CO$_2$ into sediments on similar timescales. Given the inherent assumptions built into classic carbon cycle models based on C isotope record, sedimentary Mo compilations and/or GIS mapping of known sedimentary deposits and their OC contents represent complementary methods to better characterize the global C cycle during mass extinctions and other intervals of environmental destabilization (e.g., Kemp, Suan, et al., 2022; Owens et al., 2018; *this study*). The larger estimates for the amount of organic C burial during the T-OAE calculated here also suggest that the outsized role suggested for individual basins in enhanced OC burial (and therefore "climate amelioration") may be overstated (e.g., Kemp, Suan, et al., 2022; Suan et al., 2018; see; Xu et al., 2017). Specifically, because these studies used much smaller C release estimates, the contribution of OC burial in those basins to the total global amount of OC burial is overestimated. This reasoning is also supported by paired geochemical and modeling efforts suggesting that individual European basins (and entire European realm) played a minor role in sulfide (and by corollary, OC) sequestration during the classic T-OAE interval (Gill, Lyons, & Jenkyns, 2011). A new estimation for OC burial in marine environments also supports a limited role of carbon sequestration from European basins and paleo-lakes during the T-OAE (e.g., Kemp, Suan, et al., 2022).

5. Conclusions

Increased deoxygenation, pyrite burial and possibly euxinia, and organic matter burial during the early Toarcian led to a significant drawdown of the marine Mo inventory, most likely initiated by volcanic outgassing of greenhouse gases during the emplacement of the Karoo-Ferrar LIP and subsequent biogeochemical feedbacks. The Toarcian Mo drawdown may have affected microbial ecosystems, which has ramifications for predicting the potential ecological response in future oceans to rising greenhouse gas concentrations and physical and biogeochemical feedbacks that may perturb the marine Mo (and other RSTMs) inventory. Using new data from the Fernie Formation from Canada and a global Toarcian Mo/TOC compilation, we suggest that ~41 Gt Mo and ~244,000 Gt OC were buried in marine environments during the N-CIE, which is one to two orders of magnitude larger than current estimations of C release from the Karoo-Ferrar LIP and subsequent burial in marine environments. These new Mo burial estimates suggest that at least 3% of seafloor experienced euxinic conditions during the N-CIE interval. Our OC burial estimates also support recent global redox reconstructions suggesting that widespread reducing conditions (e.g., non-sulfidic anoxia) and OC burial began in the earliest Toarcian at the Pl-To boundary (before the classic T-OAE interval and development of widespread euxinic conditions) and remained elevated well after the "OAE" ended. The term OEE better reflects the interval historically called the oceanic anoxic event. A more inclusive naming system for these CCPs is also directly applicable to OC burial in terrestrial environments as well as similar events throughout the Phanerozoic as the response to major perturbations to the Earth system were similar.

Conflict of Interest

The authors declare no conflicts of interest relevant to this study.

Data Availability Statement

The raw data can be found at https://doi.org/10.17605/OSF.IO/FH8WE.

References

Ait-Itto, F.-Z., Martinez, M., Price, G. D., & Ait Addi, A. (2018). Synchronization of the astronomical time scales in the Early Toarcian: A link between anoxia, carbon-cycle perturbation, mass extinction and volcanism. *Earth and Planetary Science Letters*, *493*, 1–11. https://doi.org/10.1016/j.epsl.2018.04.007

Algeo, T. (2004). Can marine anoxic events draw down the trace element inventory of seawater? *Geology*, *32*(12), 1057–1060. https://doi.org/10.1130/g20896.1

Algeo, T. J., & Liu, J. (2020). A re-assessment of elemental proxies for paleoredox analysis. *Chemical Geology*, *540*, 119549. https://doi.org/10.1016/j.chemgeo.2020.119549

Algeo, T. J., & Lyons, T. W. (2006). Mo–total organic carbon covariation in modern anoxic marine environments: Implications for analysis of paleoredox and paleohydrographic conditions. *Paleoceanography*, *21*(1), PA1016. https://doi.org/10.1029/2004pa001112

Algeo, T. J., & Maynard, J. B. (2004). Trace-element behavior and redox facies in core shales of Upper Pennsylvanian Kansas-type cyclothems. *Chemical Geology*, *206*(3–4), 289–318. https://doi.org/10.1016/j.chemgeo.2003.12.009

Anbar, A. D., & Knoll, A. H. (2002). Proterozoic ocean chemistry and evolution: A bioinorganic bridge? *Science*, *297*(5584), 1137–1142. https://doi.org/10.1126/science.1069651

Ardakani, O. H., Chappaz, A., Sanei, H., & Mayer, B. (2016). Effect of thermal maturity on remobilization of molybdenum in black shales. *Earth and Planetary Science Letters*, *449*, 311–320. https://doi.org/10.1016/j.epsl.2016.06.004

Baroni, I. R., Pohl, A., van Helmond, A. G. M., Papadomanolaki, N. M., Coe, A. L., Cohen, A. S., et al. (2018). Ocean circulation in the Toarcian (Early Jurassic), a key control on deoxygenation and carbon burial on the European shelf. *Paleoceanography and Paleoclimatology*, *33*(9), 994–1012. https://doi.org/10.1029/2018pa003394

Beerling, D. J., & Brentnall, S. J. (2007). Numerical evaluation of mechanisms driving Early Jurassic changes in global carbon cycling. *Geology*, *5*(3), 247–250. https://doi.org/10.1130/g23416a.1

Bennett, W. W., & Canfield, D. E. (2020). Redox-sensitive trace metals as paleoredox proxies: A review and analysis of data from modern sediments. *Earth-Science Reviews*, *204*, 103175. https://doi.org/10.1016/j.earscirev.2020.103175

Bertine, K. K., & Turekian, K. K. (1973). Molybdenum in marine deposits. *Geochimica et Cosmochimica Acta*, *37*(6), 1415–1434. https://doi.org/10.1016/0016-7037(73)90080-x

Boulila, S., Galbrun, B., Huret, E., Hinnov, L. A., Rouget, I., Gardin, S., & Bartolini, A. (2014). Astronomical calibration of the Toarcian Stage: Implications for sequence stratigraphy and duration of the early Toarcian OAE. *Earth and Planetary Science Letters*, *386*, 98–111. https://doi.org/10.1016/j.epsl.2013.10.047

Boulila, S., Galbrun, B., Sadki, D., Gardin, S., & Bartolini, A. (2019). Constraints on the duration of the early Toarcian T-OAE and evidence for carbon-reservoir change from the High Atlas (Morocco). *Global and Planetary Change*, *175*, 113–128. https://doi.org/10.1016/j.gloplacha.2019.02.005

Bowman, C. N., Them, T. R., II, Knight, M. D., Kaljo, D., Eriksson, M. E., Hints, O., et al. (2021). A multi-proxy approach to constrain locally reducing conditions in the Baltic Basin during the late Silurian (Ludfordian) Lau carbon isotope excursion. *Palaeogeography, Palaeoclimatology, Palaeoecology*, *581*, 110624. https://doi.org/10.1016/j.palaeo.2021.110624

Bowman, C. N., Young, S. A., Kaljo, D., Eriksson, M. E., Them, T. R., Hints, O., et al. (2019). Linking the progressive expansion of reducing conditions to a stepwise mass extinction event in the late Silurian oceans. *Geology*, *47*(10), 968–972. https://doi.org/10.1130/g46571.1

Breitburg, D., Levin, L. A., Oschlies, A., Grégoire, M., Chavez, F. P., Conley, D. J., et al. (2018). Declining oxygen in the global ocean and coastal waters. *Science*, *359*(6371), eaam7240. https://doi.org/10.1126/science.aam7240

Canfield, D. E. (1994). Factors influencing organic carbon preservation in marine sediments. *Chemical Geology*, *114*(3–4), 315–329. https://doi.org/10.1016/0009-2541(94)90061-2

Caruthers, A. H., Smith, P. L., & Gröcke, D. R. (2013). The Pliensbachian-Toarcian (Early Jurassic) extinction, a global multi-phased event. *Palaeogeography, Palaeoclimatology, Palaeoecology*, *386*, 104–118. https://doi.org/10.1016/j.palaeo.2013.05.010

Chappaz, A., Lyons, T. W., Gregory, D. D., Reinhard, C. T., Gill, B. C., Li, C., & Large, R. R. (2014). Does pyrite act as an important host for molybdenum in modern and ancient euxinic sediments? *Geochimica et Cosmochimica Acta*, *126*, 112–122. https://doi.org/10.1016/j.gca.2013.10.028

Chen, W., Kemp, D. B., He, T., Huang, C., Jin, S., Xiong, Y., & Newton, R. J. (2021). First record of the early Toarcian Oceanic Anoxic Event in the Hebrides Basin (UK) and implications for redox and weathering changes. *Global and Planetary Change*, *207*, 103685. https://doi.org/10.1016/j.gloplacha.2021.103685

Cohen, A. S., Coe, A. L., Harding, S. M., & Schwark, L. (2004). Osmium isotope evidence for the regulation of atmospheric CO_2 by continental weathering. *Geology*, *32*(2), 157–160. https://doi.org/10.1130/g20158.1

Dera, B., Neige, P., Dommergues, J.-L., Fara, E., Laffont, R., & Pellenard, P. (2010). High-resolution dynamics of Early Jurassic marine extinctions: The case of the Pliensbachian – Toarcian ammonites (Cephalopoda). *Journal of the Geological Society*, *167*(1), 21–33. https://doi.org/10.1144/0016-76492009-068

Diaz, R. J., & Rosenberg, R. (2008). Spreading dead zones and consequences for marine ecosystems. *Science*, *321*(5891), 926–929. https://doi.org/10.1126/science.1156401

Dickson, A. J., Gill, B. C., Ruhl, M., Jenkyns, H. C., Porcelli, D., Idiz, E., et al. (2017). Molybdenum-isotope chemostratigraphy and paleoceanography of the Toarcian Oceanic Anoxic: Event (Early Jurassic). *Geochimica et Cosmochimica Acta*, *178*, 291–306. https://doi.org/10.1016/j.gca.2019.11.001

Dickson, A. J., Idiz, E., Porcelli, D., & van den Boorn, S. H. J. M. (2020). The influence of thermal maturity on the stable isotope compositions and concentrations of molybdenum, zinc and cadmium in organic-rich marine mudrocks. *Geochimica et Cosmochimica Acta*, *287*, 205–220. https://doi.org/10.1016/j.gca.2019.11.001

Dickson, A. J., Idiz, E., Porcelli, D., Murphy, M. J., Celestino, R., Jenkyns, H. C., et al. (2022). No effect of thermal maturity on the Mo-U-Cd- and Zn-isotope compositions of Lower Jurassic organic-rich sediments. *Geology*, *50*(5), 598–602. https://doi.org/10.1130/g49724.1

Dickson, A. J., Saker-Clark, M., Jenkyns, H. C., Bottini, C., Erba, E., Russo, F., et al. (2017). A Southern Hemisphere record of global trace-metal drawdown and orbital modulation of organic-matter burial across the Cenomanian–Turonian boundary (Ocean Drilling Program Site 1138, Kerguelen Plateau). *Sedimentology*, *64*(1), 186–203. https://doi.org/10.1111/sed.12303

Emerson, S. R., & Huestead, S. S. (1991). Ocean anoxia and the concentrations of molybdenum and vanadium in seawater. *Marine Chemistry*, *34*(3–4), 177–196. https://doi.org/10.1016/0304-4203(91)90002-e

Erickson, B. E., & Helz, G. R. (2000). Molybdenum (VI) speciation in sulfidic waters. *Geochimica et Cosmochimica Acta*, *64*(7), 1149–1158. https://doi.org/10.1016/s0016-7037(99)00423-8

Fantasia, A., Föllmi, K. B., Adatte, T., Bernárdez, E., Spangenberg, J. E., & Mattioli, E. (2018). The Toarcian Oceanic Anoxic Event in south-western Gondwana: An example from the Andean Basin, northern Chile. *Journal of the Geological Society*, *175*(6), 883–902. https://doi.org/10.1144/jgs2018-008

Fantasia, A., Föllmi, K. B., Adatte, T., Spangenberg, J. E., & Montero-Serrano, J. C. (2018). The Early Toarcian oceanic anoxic event: Paleoenvironmental and paleoclimatic change across the Alpine Tethys (Switzerland). *Global and Planetary Change*, *162*, 53–68. https://doi.org/10.1016/j.gloplacha.2018.01.008

Freeman, K. H. (2001). Isotopic biogeochemistry of marine organic carbon. *Reviews in Mineralogy and Geochemistry*, *43*(1), 579–605. https://doi.org/10.2138/gsrmg.43.1.579

French, K. L., Sepúlveda, J., Trabucho-Alexandre, J., Gröcke, D. R., & Summons, R. E. (2014). Organic geochemistry of the early Toarcian oceanic anoxic event in Hawsker Bottoms, Yorkshire, England. *Earth and Planetary Science Letters*, *390*, 116–127. https://doi.org/10.1016/j.epsl.2013.12.033

Froelich, P. N., Klinkhammer, G. P., Bender, M. L., Luedtke, N. A., Heath, G. R., Cullen, D., et al. (1979). Early oxidation of organic matter in pelagic sediments of the eastern equatorial Atlantic: Suboxic diagenesis. *Geochimica et Cosmochimica Acta*, *43*(7), 1075–1090. https://doi.org/10.1016/0016-7037(79)90095-4

Gales, E., Black, B., & Elkins-Tanton, L. T. (2020). Carbonatites as a record of the carbon isotope composition of large igneous province outgassing. *Earth and Planetary Science Letters*, *535*, 116076. https://doi.org/10.1016/j.epsl.2020.116076

Gill, B. C., Dahl, T. W., Hammarlund, E. U., LeRoy, M. A., Gordon, G. W., Canfield, D. E., et al. (2021). Redox dynamics of later Cambrian oceans. *Palaeogeography, Palaeoclimatology, Palaeoecology*, *581*, 110623. https://doi.org/10.1016/j.palaeo.2021.110623

Gill, B. C., Lyons, T. W., & Jenkyns, H. C. (2011). A global perturbation to the sulfur cycle during the Toarcian oceanic anoxic event. *Earth and Planetary Science Letters*, *312*(3–4), 484–496. https://doi.org/10.1016/j.epsl.2011.10.030

Gill, B. C., Lyons, T. W., Young, S. A., Kump, L. R., Knoll, A. H., & Saltzman, M. R. (2011). Geochemical evidence for widespread euxinia in the Later Cambrian ocean. *Nature*, *469*(7328), 80–83. https://doi.org/10.1038/nature09700

Glass, J. B., Axler, R. P., Chandra, S., & Goldman, C. R. (2012). Molybdenum limitation of microbial nitrogen assimilation in aquatic ecosystems and pure cultures. *Frontiers in Microbiology*, *3*, 331. https://doi.org/10.3389/fmicb.2012.00331

Glass, J. B., Wolfe-Simon, F., Elser, J. J., & Anbar, A. D. (2010). Molybdenum—Nitrogen co-limitation in freshwater and coastal heterocystous cyanobacteria. *Limnology & Oceanography*, *55*(2), 667–676. https://doi.org/10.4319/lo.2010.55.2.0667

Goldberg, T., Poulton, S. W., Wagner, T., Kolonic, S. F., & Rehkämper, M. (2016). Molybdenum drawdown during Cretaceous oceanic anoxic event 2. *Earth and Planetary Science Letters*, *440*, 81–91. https://doi.org/10.1016/j.epsl.2016.02.006

Greber, N. D., Davies, J. H. F. L., Gaynor, S. P., Jourdan, F., Bertrand, H., & Schaltegger, U. (2020). New high precision U-Pb ages and Hf isotope data from the Karoo large igneous province; implications for pulsed magmatism and early Toarcian environmental perturbations. *Results in Geochemistry*, *1*, 100005. https://doi.org/10.1016/j.ringeo.2020.100005

Hallam, A. (2001). A review of the broad pattern of Jurassic sea-level changes and their possible causes in the light of current knowledge. *Palaeogeography, Palaeoclimatology, Palaeoecology*, *167*(1–2), 23–37. https://doi.org/10.1016/s0031-0182(00)00229-7

Hardisty, D. S., Lyons, T. W., Riedinger, N., Isson, T. T., Owens, J. D., Aller, R. C., et al. (2018). An evaluation of sedimentary molybdenum and iron as proxies for pore fluid paleoredox conditions. *American Journal of Science*, *318*(5), 527–556. https://doi.org/10.2475/05.2018.04

Harries, P., & Little, C. T. S. (1999). The early Toarcian (Early Jurassic) and Cenomanian-Turonian Late Cretaceous, mass extinctions, similarities and contrasts. *Palaeogeography, Palaeoclimatology, Palaeoecology*, *154*(1–2), 39–66. https://doi.org/10.1016/s0031-0182(99)00086-3

Hartnett, H. E., Keil, R. G., Hedges, J. I., & Devol, A. H. (1998). Influence of oxygen exposure time on organic carbon preservation in continental margin sediments. *Nature*, *391*(6667), 572–574. https://doi.org/10.1038/35351

Hermoso, M., Minoletti, F., & Pellenard, P. (2013). Black shale deposition during Toarcian super-greenhouse driven by sea level. *Climate of the Past*, *9*(6), 2703–2712. https://doi.org/10.5194/cp-9-2703-2013

Hesselbo, S. P., Gröcke, D. R., Jenkyns, H. C., Bjerrum, C. J., Farrimond, P., Morgans Bell, H. S., & Green, O. R. (2000). Massive dissociation of gas hydrate during a Jurassic oceanic anoxic event. *Nature*, *406*(6794), 392–395. https://doi.org/10.1038/35019044

Hesselbo, S. P., Little, C. T. S., Ruhl, M., Thibault, N., & Ullmann, C. V. (2020). Comments on "Paleosalinity determination in ancient epicontinental seas: A case study of the T-OAE in the Cleveland Basin (UK)" by Remirez, M. N. & Algeo, T. J. *Earth-Science Reviews*, *208*, 103290. https://doi.org/10.1016/j.earscirev.2020.103290

Ikeda, M., Hori, R. S., Ikehara, M., Miyashita, R., Chino, M., & Yamada, K. (2018). Carbon cycle dynamics linked with Karoo-Ferrar volcanism and astronomical cycles during Pliensbachian-Toarcian (Early Jurassic). *Global and Planetary Change*, *170*, 163–171. https://doi.org/10.1016/j.gloplacha.2018.08.012

Ingall, E., & Jahnke, R. (1994). Evidence for enhanced phosphorus regeneration from marine sediments overlain by oxygen depleted waters. *Geochimica et Cosmochimica Acta*, *58*(11), 2571–2575. https://doi.org/10.1016/0016-7037(94)90033-7

Izumi, K., Kemp, D. B., Itamiya, S., & Inui, M. (2018). Sedimentary evidence for enhanced hydrological cycling in response to rapid carbon release during the early Toarcian oceanic anoxic event. *Earth and Planetary Sciences*, *481*, 162–170. https://doi.org/10.1016/j.epsl.2017.10.030

Jenkyns, H. C. (1988). The early Toarcian (Jurassic) anoxic event: Stratigraphic, sedimentary, and geochemical evidence. *American Journal of Science*, *288*(2), 101–151. https://doi.org/10.2475/ajs.288.2.101

Jenkyns, H. C. (2010). Geochemistry of oceanic anoxic events. *Geochemistry, Geophysics, Geosystems*, *11*(3), Q03004. https://doi.org/10.1029/2009gc002788

Jenkyns, H. C., & Clayton, C. J. (1997). Lower Jurassic epicontinental carbonates and mudstones from England and Wales: Chemostratigraphic signals and the early Toarcian anoxic event. *Sedimentology*, *44*(4), 687–706. https://doi.org/10.1046/j.1365-3091.1997.d01-43.x

Jenkyns, H. C., Grocke, D. R., & Hesselbo, S. P. (2001). Nitrogen isotope evidence for water mass denitrification during the Early Toarcian (Jurassic) oceanic anoxic event. *Paleoceanography and Paleoclimatology*, *16*(6), 593–603. https://doi.org/10.1029/2000pa000558

Jin, X., Shi, Z., Baranyi, V., Kemp, D. B., Han, Z., Luo, G., et al. (2020). The Jenkyns Event (early Toarcian OAE) in the Ordos Basin, China. *Global and Planetary Change*, *193*, 103273. https://doi.org/10.1016/j.gloplacha.2020.103273

Keeling, R. E., Körtzinger, A., & Gruber, N. (2010). Ocean deoxygenation in a warming world. *Annual Review of Marine Science*, *2*(1), 199–229. https://doi.org/10.1146/annurev.marine.010908.163855

Kemp, D. B., & Izumi, K. (2014). Multiproxy geochemical analysis of a Panthalassic margin record of the early Toarcian oceanic anoxic event (Toyora area, Japan). *Palaeogeography, Palaeoclimatology, Palaeoecology*, *414*, 332–341. https://doi.org/10.1016/j.palaeo.2014.09.019

Kemp, D. B., Chen, W., Cho, T., Algeo, T. J., Shen, J., & Ikeda, M. (2022). Deep-ocean anoxia across the Pliensbachian-Toarcian boundary and Toarcian Oceanic Anoxic Event in the Panthalassic Ocean. *Global and Planetary Change*, *212*, 103782. https://doi.org/10.1016/j.gloplacha.2022.103782

Kemp, D. B., Selby, D., & Izumi, K. (2020). Direct coupling between carbon release and weathering during the Toarcian oceanic anoxic event. *Geology*, *48*(10), 976–980. https://doi.org/10.1130/g47509.1

Kemp, D. B., Suan, G., Fantasia, A., Jin, S., & Chen, W. (2022). Global organic carbon burial during the Toarcian oceanic anoxic event: Patterns and controls. *Earth-Science Reviews*, *231*, 104086. https://doi.org/10.1016/j.earscirev.2022.104086

Kump, L. R., & Arthur, M. A. (1999). Interpreting carbon-isotope excursions: Carbonates and organic matter. *Chemical Geology*, *161*(1–3), 181–198. https://doi.org/10.1016/s0009-2541(99)00086-8

Köhn, E. E., Münnich, M., Vogt, M., Desmet, F., & Gruber, N. (2022). Strong habitat compression by extreme shoaling events of hypoxic waters in the Eastern Pacific. *Journal of Geophysical Research: Oceans*, *127*(6), 32022JC018429. https://doi.org/10.1029/2022jc018429

Leckie, R. M., Bralower, T. J., & Cashman, R. (2002). Oceanic anoxic events and plankton evolution: Biotic response to tectonic forcing during the mid-Cretaceous. *Paleoceanography*, *17*(3), 2001PA000623. https://doi.org/10.1029/2001pa000623

Liu, M., Ji, C., Hu, H., Xia, G., Yi, H., Them, T. R., II, et al. (2021). Variations in microbial ecology during the Toarcian Oceanic Anoxic Event (Early Jurassic) in the Qiangtang Basin, Tibet: Evidence from biomarker and carbon isotopes. *Palaeogeography, Palaeoclimatology, Palaeoecology*, *580*, 110626. https://doi.org/10.1016/j.palaeo.2021.110626

Liu, M., Sun, P., Them, T. R., II, Li, Y., Sun, S., Gao, X., & Tang, Y. (2020). Organic geochemistry of a lacustrine shale across the Toarcian Oceanic Anoxic Event (Early Jurassic) from NE China. *Global and Planetary Change*, *191*, 103214. https://doi.org/10.1016/j.gloplacha.2020.103214

Long, M. C., Deutch, C., & Ito, T. (2016). Finding forced trends in oceanic oxygen. *Global Biogeochemical Cycles*, *30*(2), 381–397. https://doi.org/10.1002/2015gb005310

Lu, Z., Jenkyns, H. C., & Rickaby, R. E. M. (2010). Iodine to calcium ratios in marine carbonate as a paleo-redox proxy during oceanic anoxic events. *Geology*, *38*(12), 1107–1110. https://doi.org/10.1130/g31145.1

Lyons, T. W., Anbar, A. D., Severmann, S., Scott, C., & Gill, B. C. (2009). Tracking euxinia in the ancient ocean: A multiproxy perspective and Proterozoic case study. *Annual Review of Earth and Planetary Sciences*, *37*(1), 507–534. https://doi.org/10.1146/annurev.earth.36.031207.124233

Lyons, T. W., Reinhard, C. T., & Planavsky, N. J. (2014). The rise of oxygen in Earth's early ocean and atmosphere. *Nature*, *506*(7488), 307–315. https://doi.org/10.1038/nature13068

McArthur, J. M. (2019). Early Toarcian black shales: A response to an oceanic anoxic event or anoxia in marginal basins? *Chemical Geology*, *522*, 71–83. https://doi.org/10.1016/j.chemgeo.2019.05.028

McArthur, J. M., Algeo, T. J., van de Schootbrugge, B., Li, Q., & Howarth, R. J. (2008). Basinal restriction, black shales, Re-Os dating, and the Early Toarcian (Jurassic) oceanic anoxic event. *Paleoceanography*, *23*(4), PA4217. https://doi.org/10.1029/2008pa001607

McElwain, J., Wade-Murphy, J., & Hesselbo, S. P. (2005). Changes in carbon dioxide during an oceanic anoxic event linked to intrusion into Gondwana coals. *Nature*, *435*(7041), 479–482. https://doi.org/10.1038/nature03618

Miller, C. A., Peucker-Ehrenbrink, B., Walker, B. D., & Marcantonio, F. (2011). Re-assessing the surface cycling of molybdenum and rhenium. *Geochimica et Cosmochimica Acta*, *75*(22), 7146–7179. https://doi.org/10.1016/j.gca.2011.09.005

Monteiro, F. M., Pancost, R. D., Ridgwell, A., & Donnadieu, Y. (2012). Nutrients as the dominant control on the spread of anoxia and euxinia across the Cenomanian-Turonian oceanic anoxic event (OAE2): Model-data comparison. *Paleoceanography*, *27*(4), PA4209. https://doi.org/10.1029/2012pa002351

Morel, F. M. M., & Price, N. M. (2003). The biogeochemical cycles of trace metals in the oceans. *Science*, *300*(5621), 944–947. https://doi.org/10.1126/science.1083545

Morford, J. L., & Emerson, S. (1999). The geochemistry of redox sensitive trace metals in sediments. *Geochimica et Cosmochimica Acta*, *63*(11–12), 1735–1750. https://doi.org/10.1016/s0016-7037(99)00126-x

Newby, S. M., Owens, J. D., Schoepfer, S. D., & Algeo, T. J. (2021). Transient ocean oxygenation at end-Permian mass extinction onset shown by thallium isotopes. *Nature Geoscience*, *14*(9), 678–683. https://doi.org/10.1038/s41561-021-00802-4

Newton, R. J., Reeves, E. P., Kafousia, N., Wignall, P. B., Bottrell, S. H., & Sha, J.-G. (2011). Low marine sulfate concentrations and the isolation of the European epicontinental sea during the Early Jurassic. *Geology*, *39*(1), 7–10. https://doi.org/10.1130/g31326.1

Nielsen, S. G., Goff, M., Hesselbo, S. P., Jenkyns, H. C., LaRowe, D. E., & Lee, C.-T. A. (2011). Thallium isotopes in early diagenetic pyrite–A paleoredox proxy? *Geochimica et Cosmochimica Acta*, *77*(21), 6690–6704. https://doi.org/10.1016/j.gca.2011.07.047

Ostrander, C. M., Owens, J. D., & Nielsen, S. G. (2017). Constraining the rate of oceanic deoxygenation leading up to a Cretaceous Oceanic Anoxic Event (OAE-2: ∼94 Ma). *Science Advances*, *3*(8), e1701020. https://doi.org/10.1126/sciadv.1701020

Owens, J. D. (2019). Application of thallium isotopes: Tracking marine oxygenation through manganese oxide burial. In *Elements in geochemical tracers in Earth system science*. Cambridge University Press.

Owens, J. D., Gill, B. C., Jenkyns, H. C., Bates, S. M., Severmann, S., Kuypers, M. M. M., et al. (2013). Sulfur isotopes track the extent and dynamics of euxinia during Cretaceous Oceanic Anoxic Event 2. *Proceedings of the National Academy of Sciences*, *110*(46), 18407–18412. https://doi.org/10.1073/pnas.1305304110

Owens, J. D., Lyons, T. W., & Lowery, C. M. (2018). Quantifying the missing sink for global organic carbon burial during a Cretaceous oceanic anoxic event. *Earth and Planetary Science Letters*, *499*, 83–94. https://doi.org/10.1016/j.epsl.2018.07.021

Owens, J. D., Reinhard, C. T., Rohrssen, M., Love, G. D., & Lyons, T. W. (2016). Empirical links between trace metal cycling and marine microbial ecology during a large perturbation to Earth's carbon cycle. *Earth and Planetary Science Letters*, *449*, 407–417. https://doi.org/10.1016/j.epsl.2016.05.046

Pană, D., Poulton, T. P., & DrFrane, S. A. (2019). U-Pb detrital zircon dating supports Early Jurassic initiation of the Cordilleran foreland basin in southwestern Canada. *GSA Bulletin*, *13*(1/2), 318–334. https://doi.org/10.1130/b31862.1

Partin, C. A., Bekker, A., Planavsky, N. J., Scott, C. T., Gill, B. C., Li, C., et al. (2013). Large-scale fluctuations in Precambrian atmospheric and oceanic oxygen levels from the record of U in shales. *Earth and Planetary Science Letters*, *369–370*, 284–293. https://doi.org/10.1016/j.epsl.2013.03.031

Pearce, C. R., Cohen, A. S., Coe, A. L., & Burton, K. W. (2008). Molybdenum isotope evidence for global ocean anoxia coupled with perturbations to the carbon cycle during the Early Jurassic. *Geology*, *36*(3), 231–234. https://doi.org/10.1130/g24446a.1

Percival, L. M. E., Cohen, A. S., Davies, M. K., Dickson, A. J., Hesselbo, S. P., Jenkyns, H. C., et al. (2016). Osmium isotope evidence for two pulses of increased continental weathering linked to Early Jurassic volcanism and climate change. *Geology*, *44*(9), 759–762. https://doi.org/10.1130/g37997.1

Poulton, T. P., & Aitken, J. D. (1989). The Lower Jurassic phosphorites of southeastern British Columbia and terrane accretion to western North America. *Canadian Journal of Earth Sciences*, *26*(8), 1612–1616. https://doi.org/10.1139/e89-137

Pálfy, J., & Smith, P. L. (2000). Synchrony between Early Jurassic extinction, oceanic anoxic event, and the Karoo-Ferrar flood basalt volcanism. *Geology*, *28*(8), 747–750. https://doi.org/10.1130/0091-7613(2000)028<0747:sbejeo>2.3.co;2

Reinhard, C. T., Planavsky, N. J., Robbins, L. H., Partin, C. A., Gill, B. C., Lalonde, S. V., et al. (2013). Proterozoic ocean redox and biogeochemical stasis. *Proceedings of the National Academy of Sciences*, *110*(14), 5357–5362. https://doi.org/10.1073/pnas.1208622110

Remírez, M. N., & Algeo, T. J. (2020a). Carbon-cycle changes during the Toarcian (Early Jurassic) and implications for regional versus global drivers of the Toarcian oceanic anoxic event. *Earth-Science Reviews*, *209*, 103283. https://doi.org/10.1016/j.earscirev.2020.103283

Remírez, M. N., & Algeo, T. J. (2020b). Paleosalinity determination in ancient epicontinental seas: A case study of the T-OAE in the Cleveland Basin (UK). *Earth-Science Reviews*, *201*, 103072. https://doi.org/10.1016/j.earscirev.2019.103072

Ruebsam, W., Mayer, B., & Schwark, L. (2019). Cryosphere carbon dynamics control early Toarcian global warming and sea level evolution. *Global and Planetary Change*, *172*, 440–453. https://doi.org/10.1016/j.gloplacha.2018.11.003

Ruebsam, W., Reolid, M., & Schwark, L. (2020). $\delta^{13}C$ of terrestrial vegetation records Toarcian CO_2 and climate gradients. *Scientific Reports*, *10*(1), 117. https://doi.org/10.1038/s41598-019-56710-6

Schlanger, S. O., & Jenkyns, H. C. (1976). Cretaceous oceanic anoxic events: Causes and consequences. *Geologie en Mijnbouw*, *55*, 179–184.

Schmidtko, S., Stramma, L., & Visbeck, M. (2017). Decline in global oceanic oxygen content during the past five decades. *Nature*, *542*(7641), 335–339. https://doi.org/10.1038/nature21399

Schouten, S., van Kaam-Peters, H. M. E., Rijpstra, W. I. C., Schoell, M., & Damsté, J. S. S. (2000). Effects of an oceanic anoxic event on the stable carbon isotopic composition of early Toarcian carbon. *American Journal of Science*, *300*, 1–22. https://doi.org/10.2475/ajs.300.1.1

Schwark, L., & Frimmel, A. (2004). Chemostratigraphy of the Posidonia Black Shale, SW Germany II. Assessment of extent and persistence of photic-zone anoxia using aryl isoprenoid distributions. *Chemical Geology*, *206*(3–4), 231–248. https://doi.org/10.1016/j.chemgeo.2003.12.008

Scotese, C. R. (2001). *Atlas of Earth history*. PALEOMAP Project.

Scott, C., & Lyons, T. W. (2012). Contrasting molybdenum cycling and isotopic properties in euxinic versus non-euxinic sediments and sedimentary rocks: Refining the paleoproxies. *Chemical Geology*, *324–325*, 19–27. https://doi.org/10.1016/j.chemgeo.2012.05.012

Scott, C., Lyons, T. W., Bekker, A., Shen, Y., Poulton, S. W., Chu, X., & Anbar, A. D. (2008). Tracing the stepwise oxygenation of the Proterozoic ocean. *Nature*, *452*(7186), 456–459. https://doi.org/10.1038/nature06811

Sell, B., Ovtcharova, M., Guex, J., Bartolini, A., Jourdan, F., Spangenberg, J. E., et al. (2014). Evaluating the temporal link between the Karoo LIP and climatic–biologic events of the Toarcian Stage with high-precision U–Pb geochronology. *Earth and Planetary Science Letters*, *408*, 48–56. https://doi.org/10.1016/j.epsl.2014.10.008

Shimmield, G. B., & Price, N. B. (1986). The behaviour of molybdenum and manganese during early sediment diagenesis — Offshore Baja California, Mexico. *Marine Chemistry*, *19*(3), 261–280. https://doi.org/10.1016/0304-4203(86)90027-7

Suan, G., Schöllhorn, I., Schlögl, J., Segit, J., Mattioli, E., Lécuyer, C., & Fourel, F. (2018). Euxinic conditions and high sulfur burial near the European shelf margin (Pieniny Klippen Belt, Slovakia) during the Toarcian oceanic anoxic event. *Global and Planetary Change*, *170*, 246–259. https://doi.org/10.1016/j.gloplacha.2018.09.003

Takematsu, N., Sato, Y., Okabe, S., & Nakayama, E. (1985). The partition of vanadium and molybdenum between manganese oxides and sea water. *Geochimica et Cosmochimica Acta*, *49*(11), 2395–2399. https://doi.org/10.1016/0016-7037(85)90239-x

Them, T. R., Gill, B. C., Selby, D., Gröcke, D. R., Friedman, R. M., & Owens, J. D. (2017). Evidence for rapid weathering response to climatic warming during the Toarcian Oceanic Anoxic Event. *Scientific Reports*, *7*(1), 5003. https://doi.org/10.1038/s41598-017-05307-y

Them, T. R., II, Gill, B. C., Caruthers, A. H., Gerhardt, A. M., Gröcke, D. R., Lyons, T. W., et al. (2018). Thallium isotopes reveal protracted anoxia during the Toarcian (Early Jurassic) associated with volcanism, carbon burial, and mass extinction. *Proceedings of the National Academy of Sciences*, *115*(26), 6596–6601. https://doi.org/10.1073/pnas.1803478115

Them, T. R., II, Gill, B. C., Caruthers, A. H., Gröcke, D. R., Tulsky, E. T., Martindale, R. C., et al. (2017). High-resolution carbon isotope records of the Toarcian Oceanic Anoxic Event (Early Jurassic) from North America and implications for the global drivers of the Toarcian carbon cycle. *Earth and Planetary Science Letters*, *459*, 118–126. https://doi.org/10.1016/j.epsl.2016.11.021

Them, T. R., II, Jagoe, C. H., Caruthers, A. H., Gill, B. C., Grasby, S. E., Gröcke, D. R., et al. (2019). Terrestrial sources as the primary delivery mechanism of mercury to the oceans across the Toarcian Oceanic Anoxic Event (Early Jurassic). *Earth and Planetary Science Letters*, *507*, 62–72. https://doi.org/10.1016/j.epsl.2018.11.029

Thibault, N., Ruhl, M., Ullmann, C. V., Korte, C., Kemp, D. B., Gröcke, D. R., & Hesselbo, S. P. (2018). The wider context of the Lower Jurassic Toarcian oceanic anoxic event in Yorkshire coastal outcrops, UK. *Proceedings of the Geologists' Association*, *29*(3), 372–391. https://doi.org/10.1016/j.pgeola.2017.10.007

Tribovillard, N., Algeo, T. J., Lyons, T., & Riboulleau, A. (2006). Trace metals as paleoredox and paleoproductivity proxies: An update. *Chemical Geology*, *232*(1–2), 12–32. https://doi.org/10.1016/j.chemgeo.2006.02.012

Ullmann, C. V., Boyle, R., Duarte, L. V., Hesselbo, S. P., Kasemann, S. A., Klein, T., et al. (2020). Warm afterglow from the Toarcian Oceanic Anoxic Event drives the success of deep-adapted brachiopods. *Scientific Reports*, *10*(1), 6549. https://doi.org/10.1038/s41598-020-63487-6

van Breugal, Y., Baas, M., Schouten, S., Mattioli, E., & Damsté, J. S. S. (2006). Isorenieratane record in black shales from the Paris Basin, France: Constraints on recycling of respired CO_2 as a mechanism for negative carbon isotope shifts during the Toarcian oceanic anoxic event. *Paleoceanography*, *21*(4), PA4220. https://doi.org/10.1029/2006pa001305

Wang, Y., Ossa Ossa, F., Spangenberg, J. E., Wille, M., & Schoenberg, R. (2021). Restricted oxygen-deficient basins on the northern European epicontinental shelf across the Toarcian carbon isotope excursion interval. *Paleoceanography and Paleoclimatology*, *36*(6), e2020PA004207. https://doi.org/10.1029/2020PA004207

Xu, W., Ruhl, M., Jenkyns, H. C., Hesselbo, S. P., Riding, J. B., Selby, D., et al. (2017). Carbon sequestration in an expanded lake system during the Toarcian oceanic anoxic event. *Nature Geoscience*, *10*(2), 129–134. https://doi.org/10.1038/ngeo2871

Xu, W., Ruhl, M., Jenkyns, H. C., Leng, M. J., Huggett, J. M., Minisini, D., et al. (2018). Evolution of the Toarcian (Early Jurassic) carbon-cycle and global climatic controls on local sedimentary processes (Cardigan Bay Basin, UK). *Earth and Planetary Science Letters*, *484*, 396–411. https://doi.org/10.1016/j.epsl.2017.12.037